

## **CHAPTER FOUR: RESULTS AND DISCUSSIONS**

This chapter consists of the simulation results of the plug flow reactors of two different scenarios.



University of Moratuwa, Sri Lanka.  
Electronic Theses & Dissertations  
[www.lib.mrt.ac.lk](http://www.lib.mrt.ac.lk)

## 4. Results and discussions

This section reveals the simulation results of plug flow reactor relevant to two modeling scenarios.

### 4.1 Results from first plug flow reactor model (1<sup>st</sup> scenario)

This section investigates the characteristic behavior of plug flow reactor under various organic loading rates.

#### 4.1.1 Feed rate

The reactor is fed continuously throughout the simulation under different feeding rates in order to maintain different retention times. Figure 4-1 shows the feed pattern of plug flow reactor under different HRT in days.

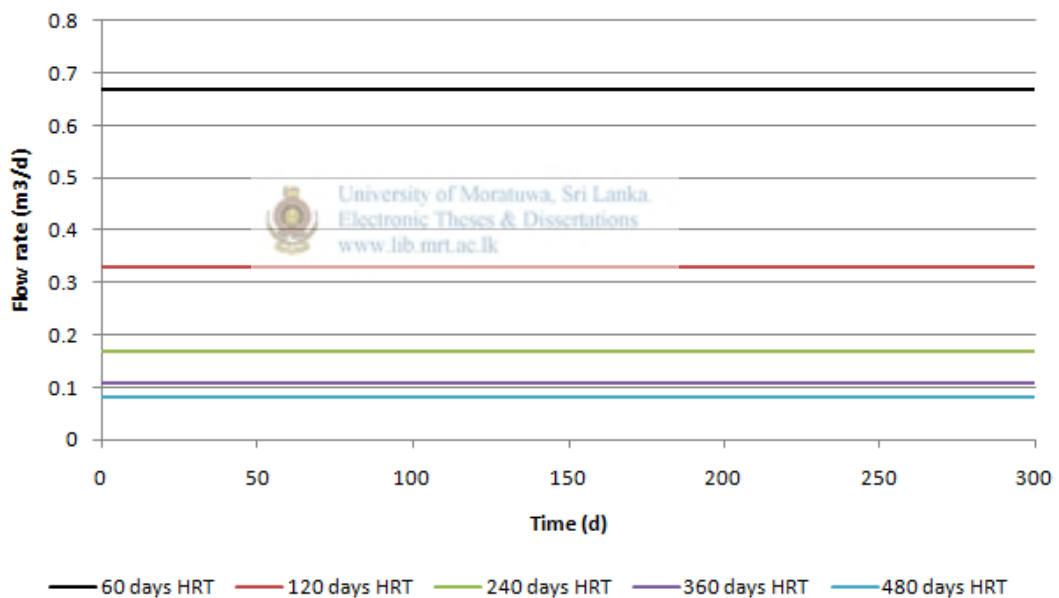


Figure 4-1: Reactor Feed rates

#### 4.1.2 Gas production rate and composition

The rate of gas production was observed by changing the feed rate of the reactor. The Figure 4-2 shows the gas production rate under different feed rates.

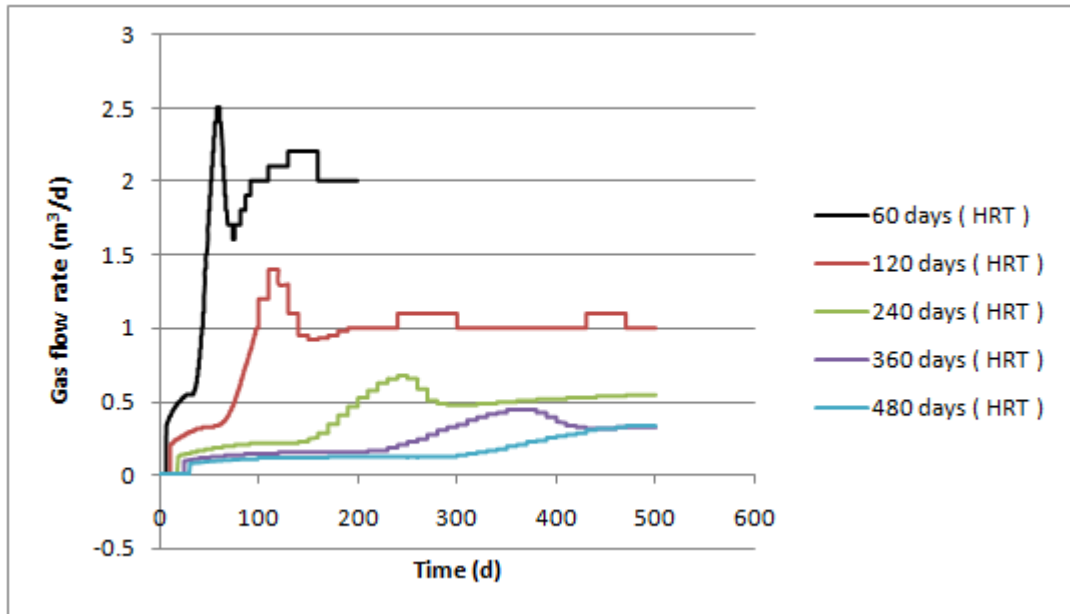


Figure 4-2: Variation of gas rate in PFR under different feed rates

According to the Figure 4-2 a high gas production can be observed under low retention times. The gas production rate is at its optimum value under HRT of 60 days. Gas production rate gradually decreases with increase of HRT and become a minimum under HRT of 480 days. The digested slurry comes to the slurry tanks after the reactor operating time reaches the reactor retention time (1-HRT). The results of the gas composition shows that methane composition decreases drastically after the reactor operating time reaches the HRT of the reactor. It is due to the lack of methane in the slurry at the exit of plug flow reactor. At the same time both carbon dioxide and hydrogen percentage of the gas mixture increases.

Figure 4-3 shows that the variation of gas composition of plug flow reactor at 60 days HRT. Methane composition decreases from the beginning of the reactor operation and it converts to a rapid decrease after reactor operating time reach the reactor retention time (HRT) of the reactor. At the same time compositions of both carbon dioxide and hydrogen start to increase.

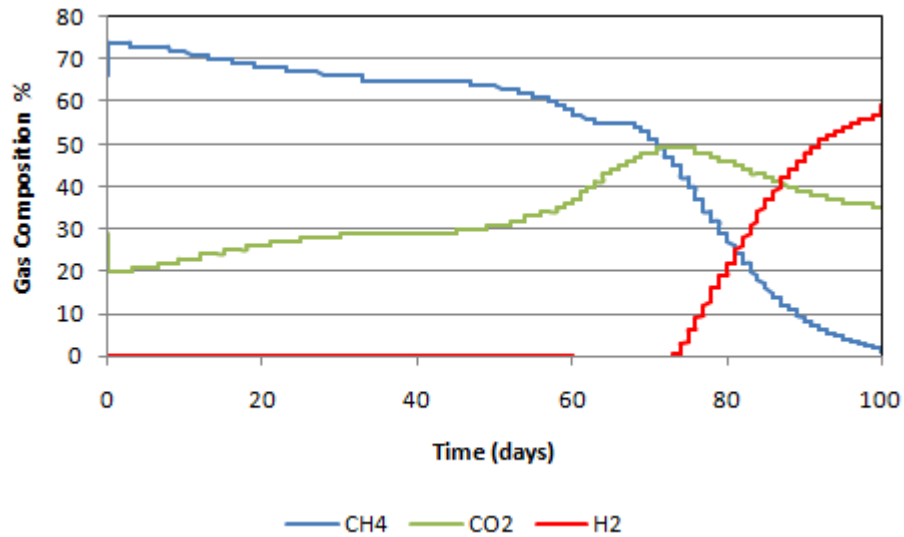


Figure 4-3: Variation of gas composition in PFR with 60 HRT

Figure 4-4 shows the variation of gas composition of plug flow reactor having 120 days HRT. As in the figure 4-3 composition of methane decreases from the beginning of the reactor operation and it converts to a rapid decrease after simulation time reach the reactor retention time 120 days. At the same time compositions of both carbon dioxide and hydrogen start to increase.

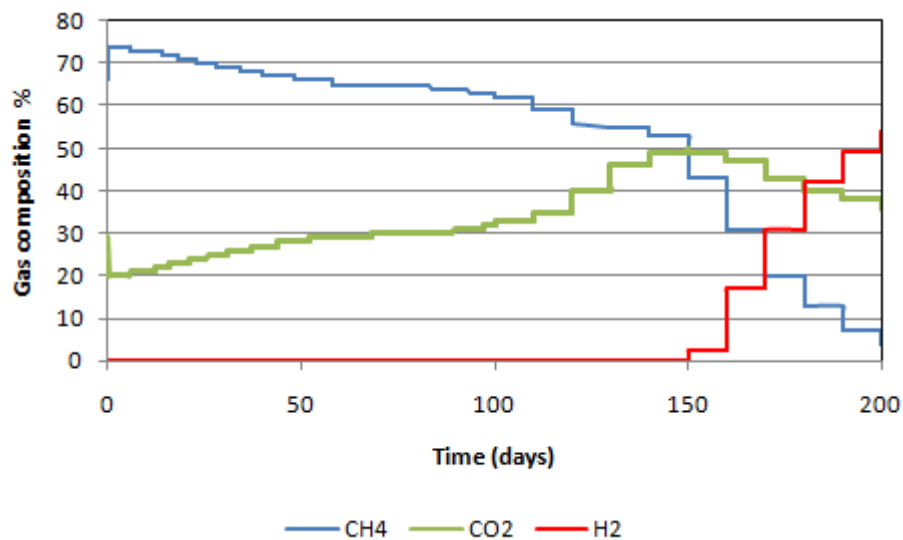


Figure 4-4: Variation of gas composition in PFR with 120 HRT

Figure 4-5 shows the variation of gas composition of plug flow reactor having 240 days HRT. Similarly a sudden drop of methane composition was observed after time reached to reactor retention time of 240 days.

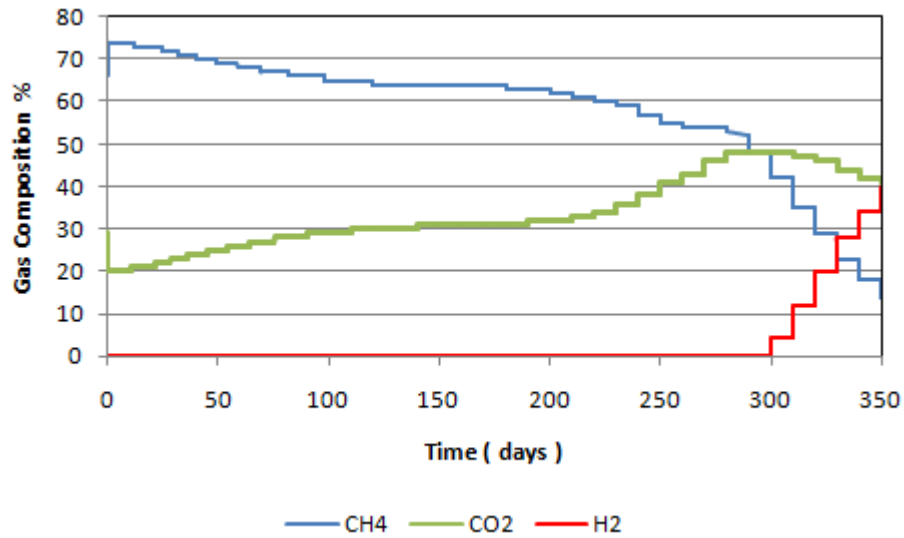


Figure 4-5: Variation of gas composition in PFR with 240 HRT

Figure 4-6 shows the variation of gas composition of plug flow reactor having 360 days HRT. Same variation in methane composition showed under each and every feed condition. Rapid change of compositions started after the time of 360 days.

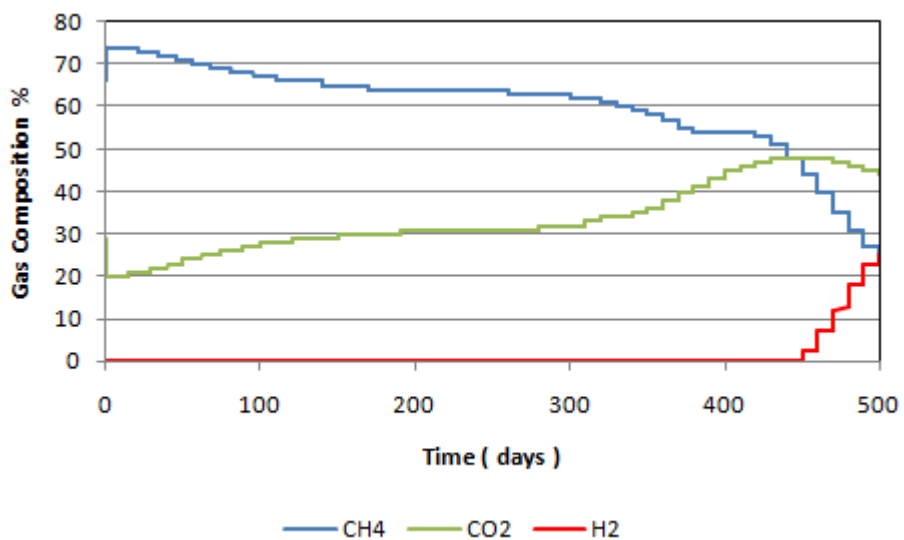


Figure 4-6: Variation of gas composition in PFR with 360 HRT

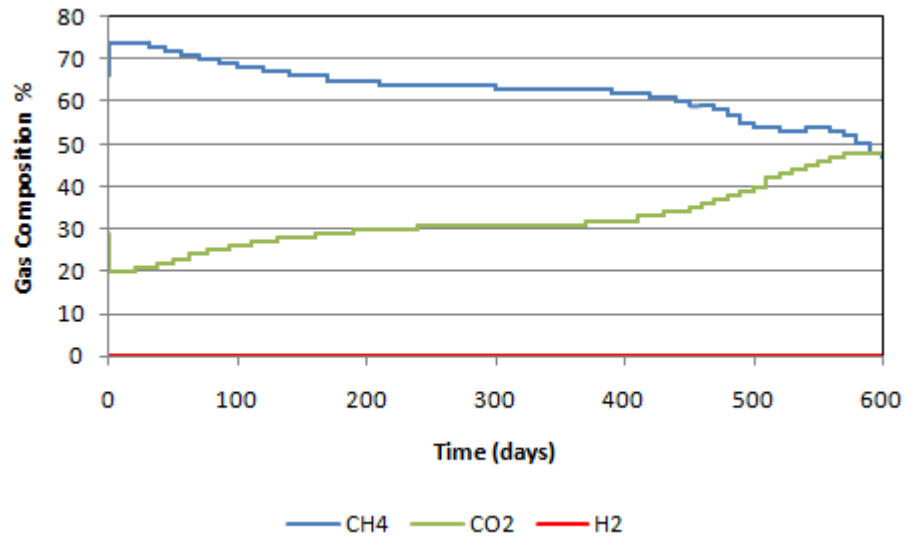


Figure 4-7: Variation of gas composition in PFR with 480 HRT

Figure 4-7 shows the variation of gas composition of plug flow reactor having 480 days HRT.

#### 4.1.3 Variations in soluble gases along the reactor

The variation of soluble gases along the reactor was shown in following figures. Here the main concern was given to the dissolve methane content of the slurry.

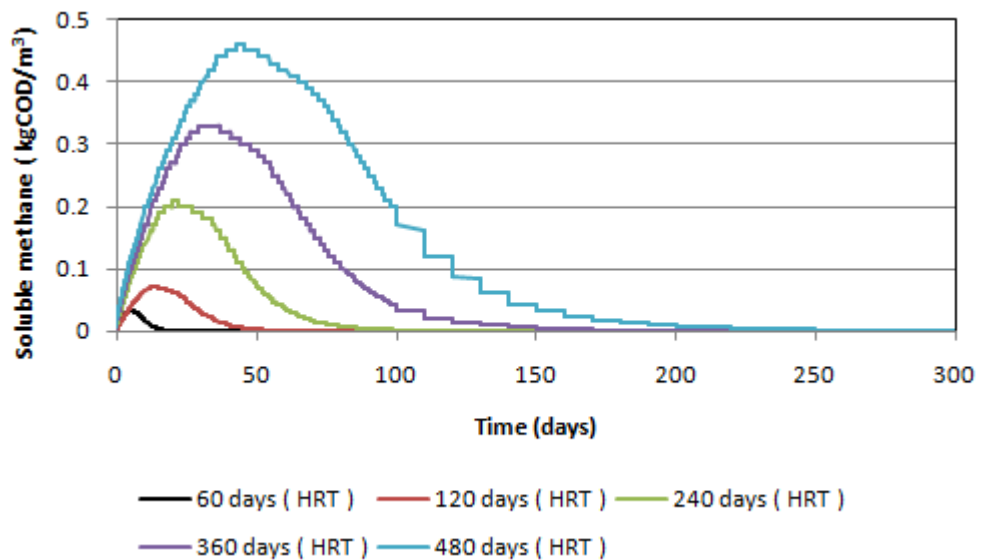


Figure 4-8: Dissolve methane concentration at the Plug flow reactor front

Figure 4-8 shows the variation of dissolve methane at the front of the reactor. At every feed rate, the dissolved methane concentration goes to a maximum level. The value corresponds to maximum level increases when the feed rate decreases.

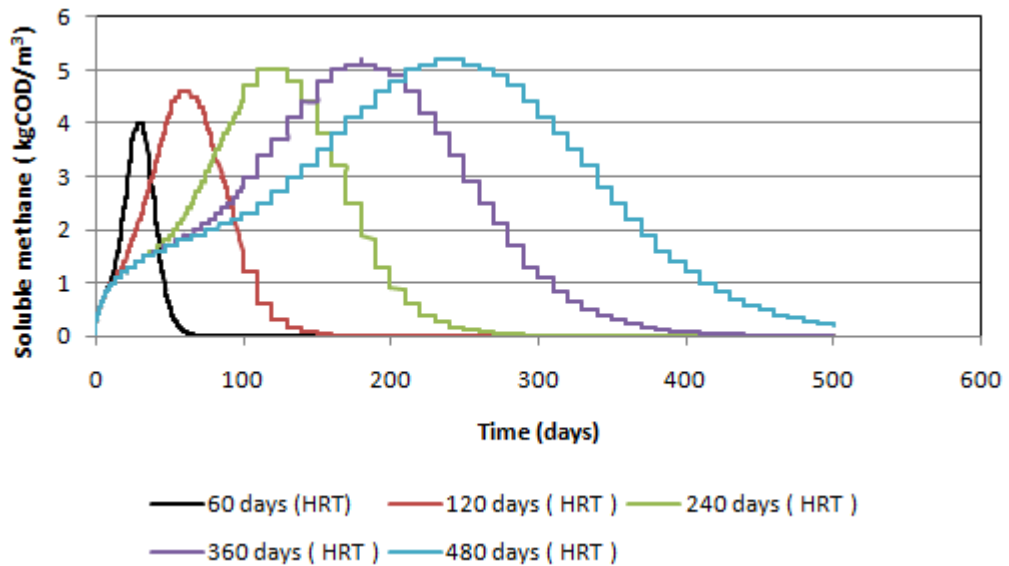


Figure 4-9: Dissolve methane concentration at the plug flow reactor middle

At the middle of the plug flow reactor the optimum values of dissolve methane are much higher than that of at the front of the reactor. Figure 4-9 shows the variation of dissolved methane at the middle of the reactor.

Figure 4-10 shows the variation of dissolve methane at the end of the reactor. Optimum dissolved level of methane comes almost same for every feed rate.

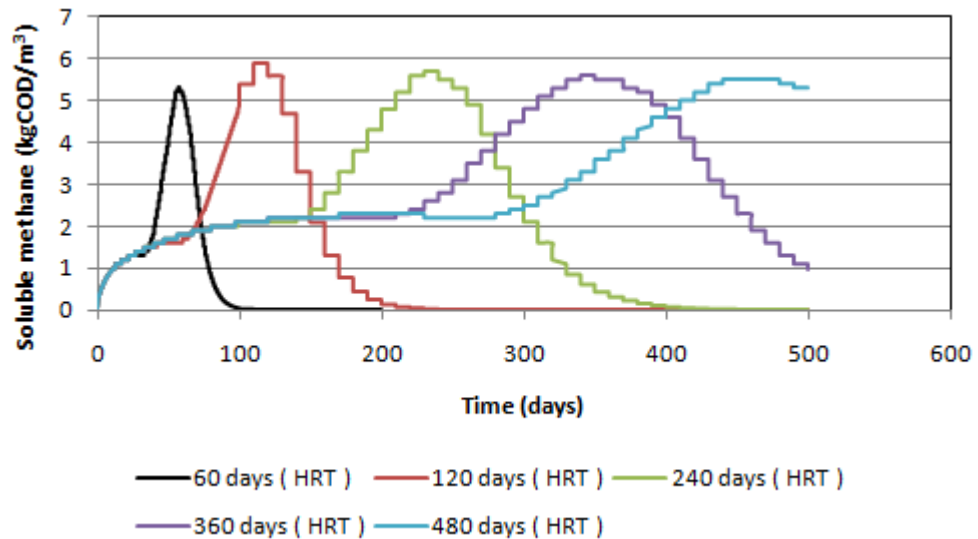
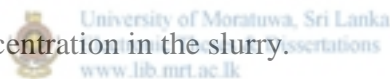


Figure 4-10: Dissolve methane concentration at the plug flow reactor end

The Advective - Diffusive reactor compartment in AQUASIM 2.1f does not allow building a diffusive link in order to transfer any gas produced within reactor to a gaseous phase. Owing to this, all the gas produced during the digestion dissolved in slurry of the reactor. Dissolution of excess amount of methane leads to increase the dissolve methane concentration in the slurry.



#### 4.1.4 VFA variation along the reactor

The figures show the variation of the volatile fatty acids within the reactor compartment in different locations under different feed rates. Figure 4-11 shows the TVFA variation at the front of the reactor.

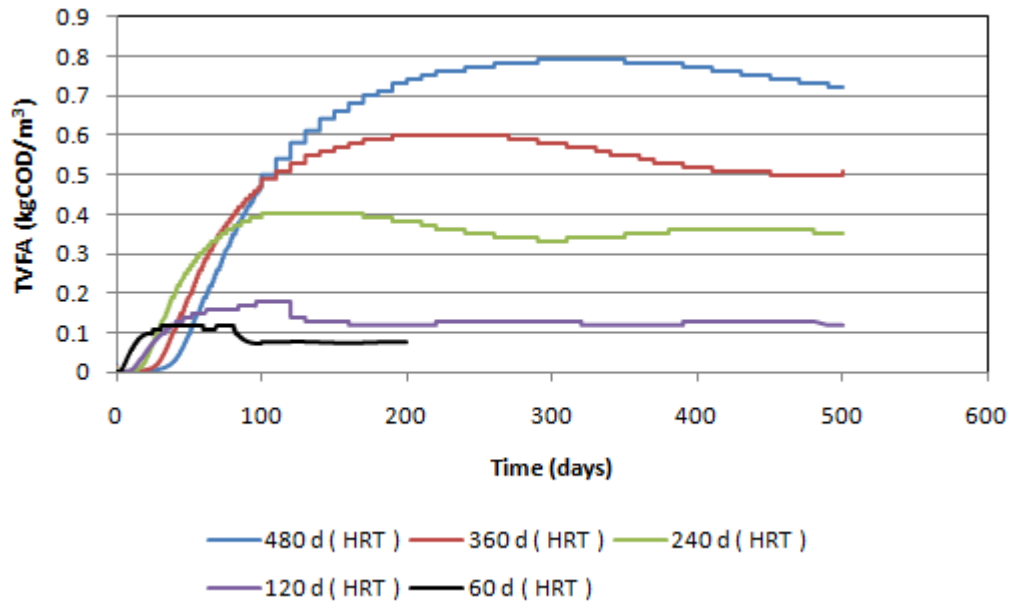


Figure 4-11: Total VFA variation at the front of the reactor

As far as reactor front is concerned the concentration of TVFA increases in to a higher value for the large retention time. There is a high rate of production of VFA in lowest retention time. VFA production rate decreases with the increase of reactor retention time. Under low retentions high amount of substrate is added to the reactor. Therefore the rate of VFA formation is high under the low retention times. The maximum TVFA concentration is low in high feed rates and gradually increased when decreasing feed rate. This is due to the high rate of feed transfer through the reactor under high flow rates. Under low flow rates feed do not transfer in significant rate. Thus there is enough time to increase the VFA concentration at the front of plug flow reactor under low flow rates.

Figure 4-12 shows the variation of TVFA at the middle of the reactor. The same variation can be observed here in TVFA increases as in front of the plug flow reactor but finally TVFA reach to an optimum value of 8 kgCOD/m<sup>3</sup>.

There is no significant variation of TVFA at the end of the reactor until the feed transfer to that point. Once TVFA transferred it starts to increase and comes to an optimum value as shown in the Figure 4-13.

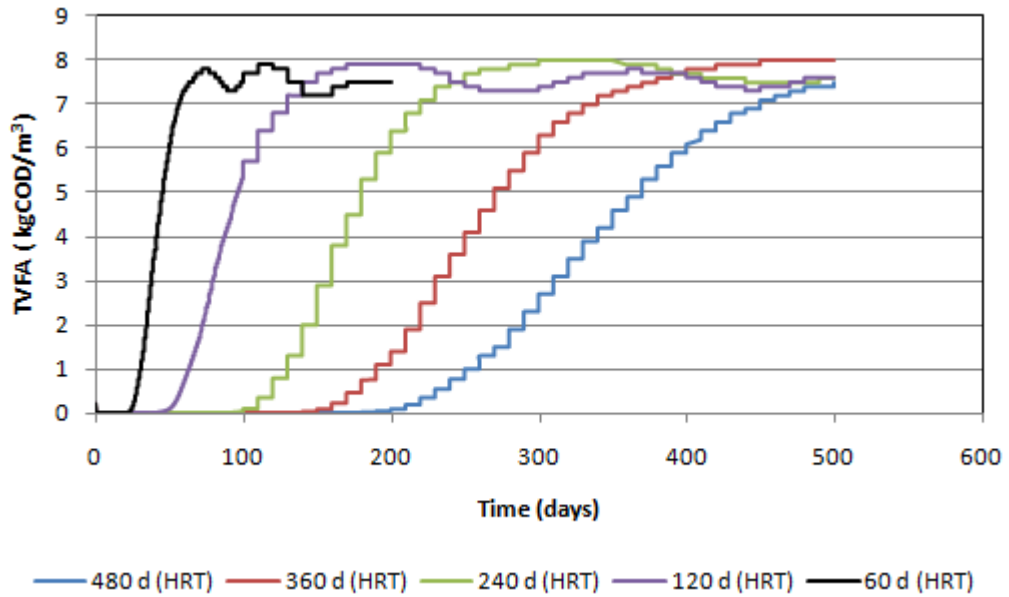


Figure 4-12: Total VFA variation at the middle of the reactor

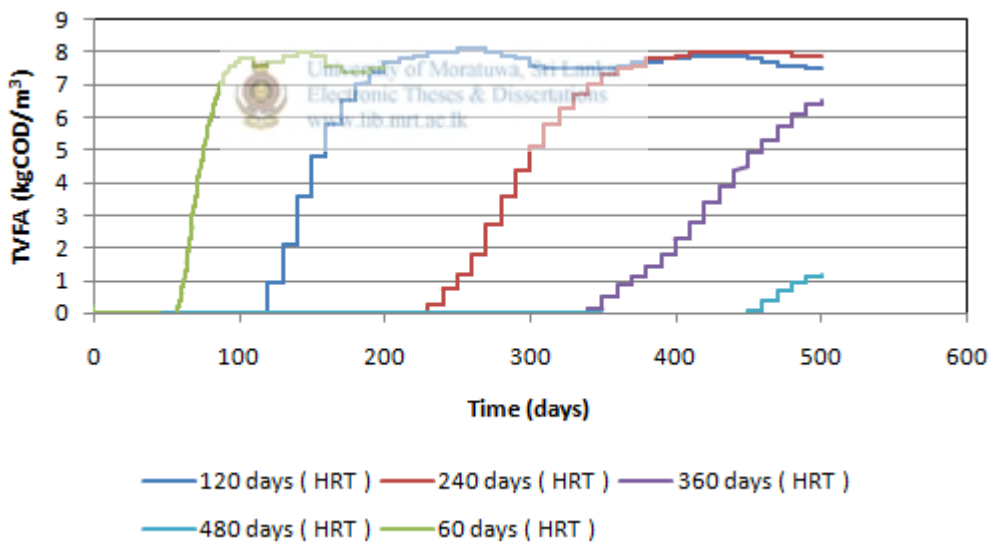


Figure 4-13: Total VFA variation at the end of the reactor

#### 4.1.5 Variation of pH along the reactor

The variation of pH was observed at the front, middle and end of the reactor. Figure 4-14 shows the pH variation at the front under different retention times. There, high

pH drop observed under lowest retention. Reduction of pH decreased with the increase of retention time in reactor. Low retention resulting high TVFA production at the front. High rate of increase of VFA concentration causes a rapid pH drop at the front of the plug flow reactor. Reduction of pH reduces with the decreases of VFA concentration variation in the reactor. Figure 4-15 and Figure 4-16 show the pH variation at the middle and the end of plug flow reactor under different retention times.

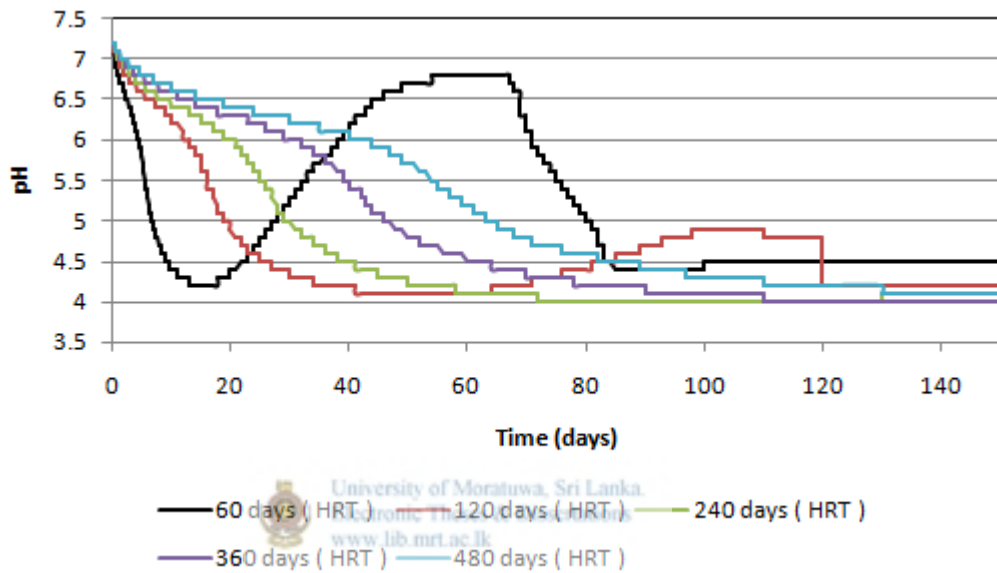


Figure 4-14: pH variation of the plug flow reactor at front

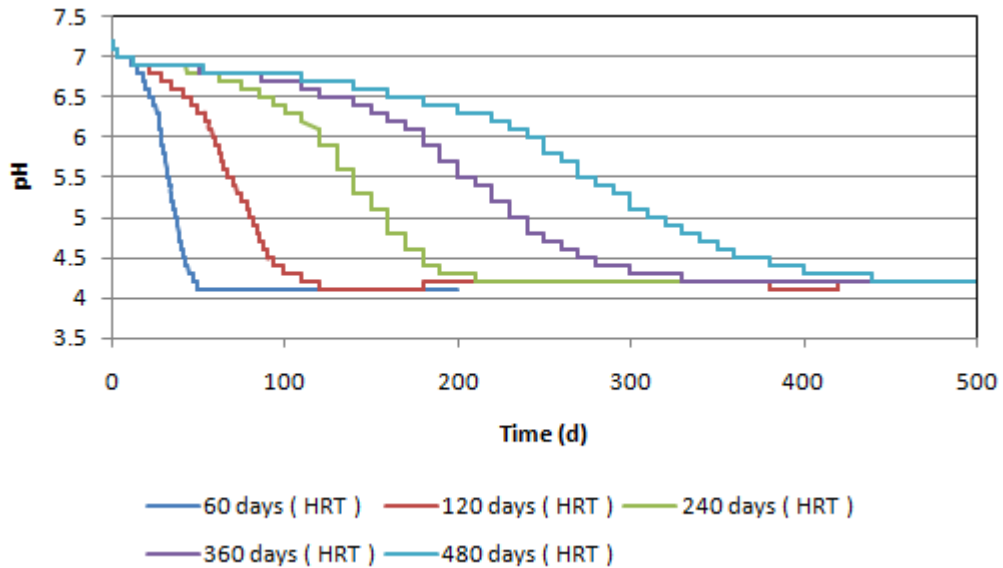


Figure 4-15: pH variation of the plug flow reactor at middle

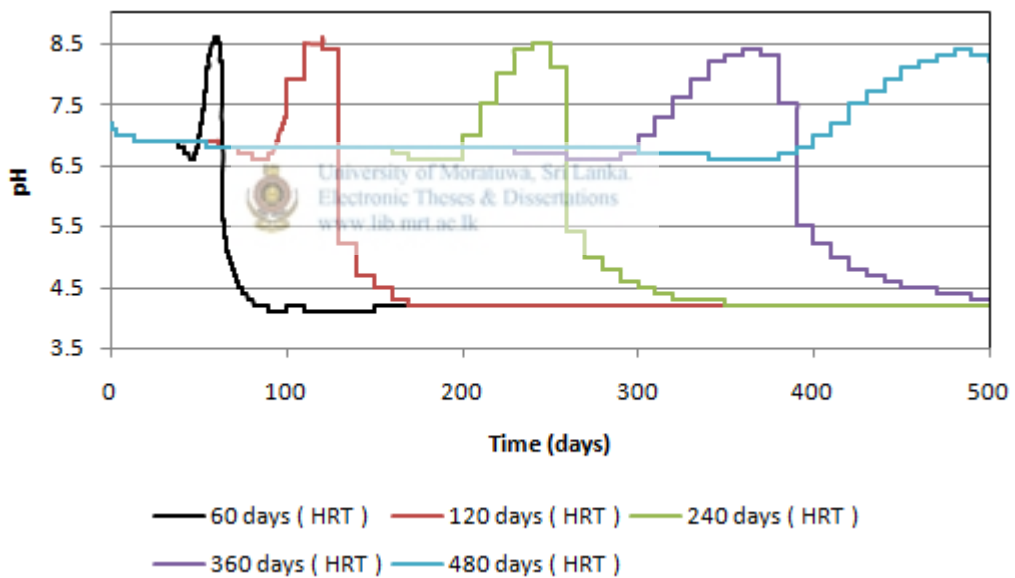


Figure 4-16: pH variation of the plug flow reactor at end

#### 4.1.6 Variations of inhibition functions along the reactor

The reactor undergoes a rapid pH reduction in the slurry. High rate of conversion of organic fraction into VFA has caused this consequence. pH inhibits the methanogenesis phase in the reactor. Inhibitions lead to stop the conversion of acetate and hydrogen to methane. It will continue at both the middle and the end of

the reactor. With the termination of the methanogenic process the concentrations of acetates and the hydrogen increase in the reactor.

Several inhibitions were analyzed as pH inhibition of acetogens and acidogens, hydrogen utilizing methanogens and acetoclastic methanogens, hydrogen inhibition of acetogenic bacteria and ammonia inhibition of acetoclastic methanogens along the reactor. A significant variation of inhibition functions were observed under different reactor feed rates.

#### **4.1.6.1 pH inhibition of acetate degrading organisms**

pH is a main factor which causes to inhibition of microorganism in anaerobic digestion. Sudden reduction of pH was observed at the reactor front under given feed conditions. Figure 4-14 shows the variation of pH at the reactor front under different feed rates. Accordingly the value of the inhibition function of acetate degrading organisms shows a rapid reduction and eventually comes to zero. The reduction of pH decreases under low feed rate conditions and a rapid reduction of pH was observed with the increase of feed rate. Consequently pH inhibition of acetate degrading organisms reduced with decrease of feed rate. Similar type of inhibition of acetate degrading organisms shows at reactor middle as well but the variation is not rapid as at reactor front. Figure 4-17 and Figure 4-18 shows the variation of inhibition function at reactor front and middle.

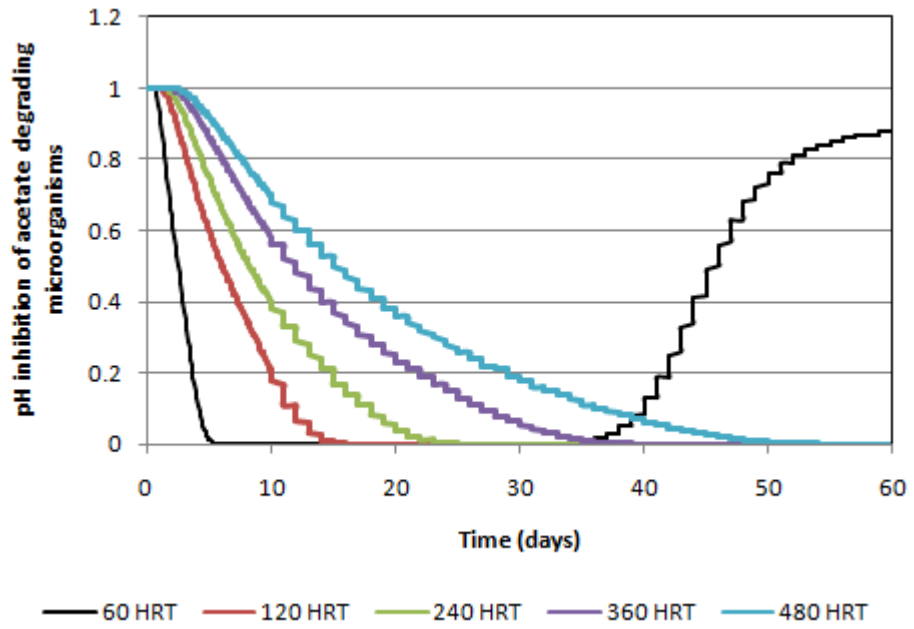


Figure 4-17 : pH inhibition of acetate degrading microorganisms at reactor front

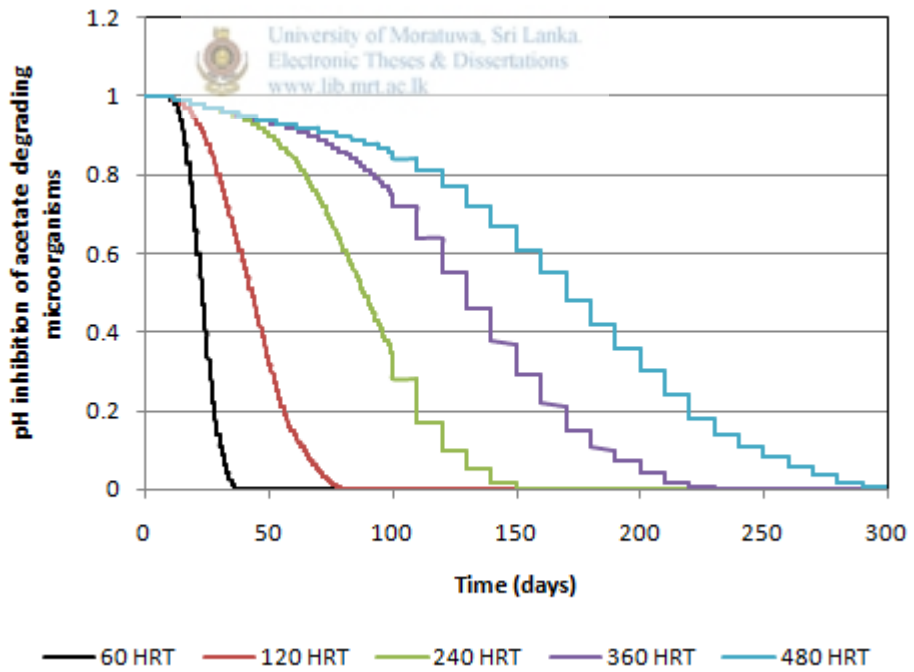


Figure 4-18: pH inhibition of acetate degrading microorganisms at reactor middle

#### 4.1.6.2 pH inhibition of acetogens and acidogens

pH causes to inhibit the growth of acetogens and acidogens in AD. A rapid inhibition of acetogens and acidogens were observed with the time at the reactor front and ultimately it comes to a steady value of approximately 0.1. The Figure 4-19 shows the variation of the inhibition function at the front of the reactor. In here the inhibition decreases along the reactor. Figure 4-20 shows the variation of the inhibition function at the middle of the reactor. At the reactor middle, the rate of decrease of pH is not very much higher as at front. This results a reduction in inhibition of acetogens and acidogens at the reactor middle.

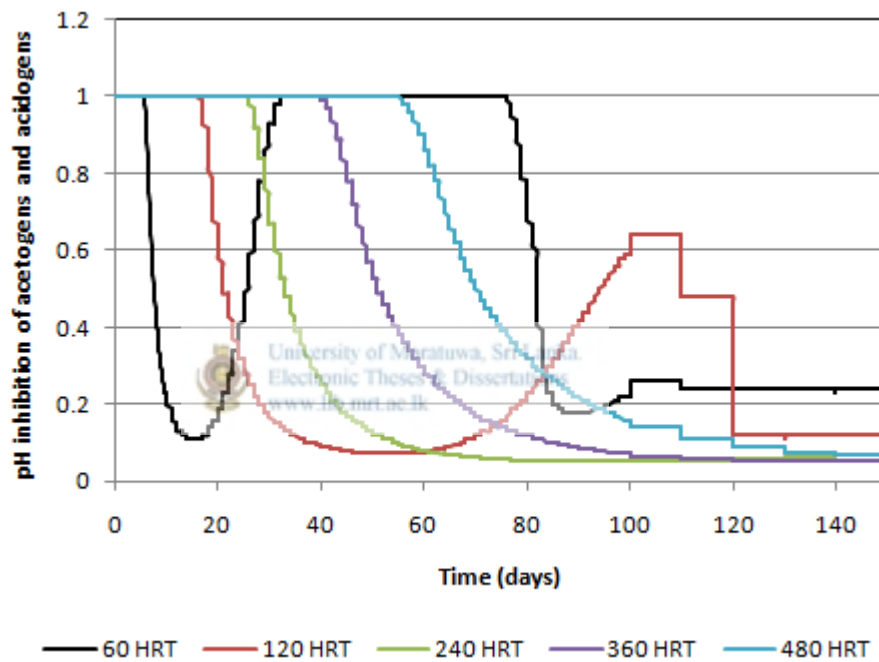


Figure 4-19: pH inhibition of acetogens and acidogens at reactor front

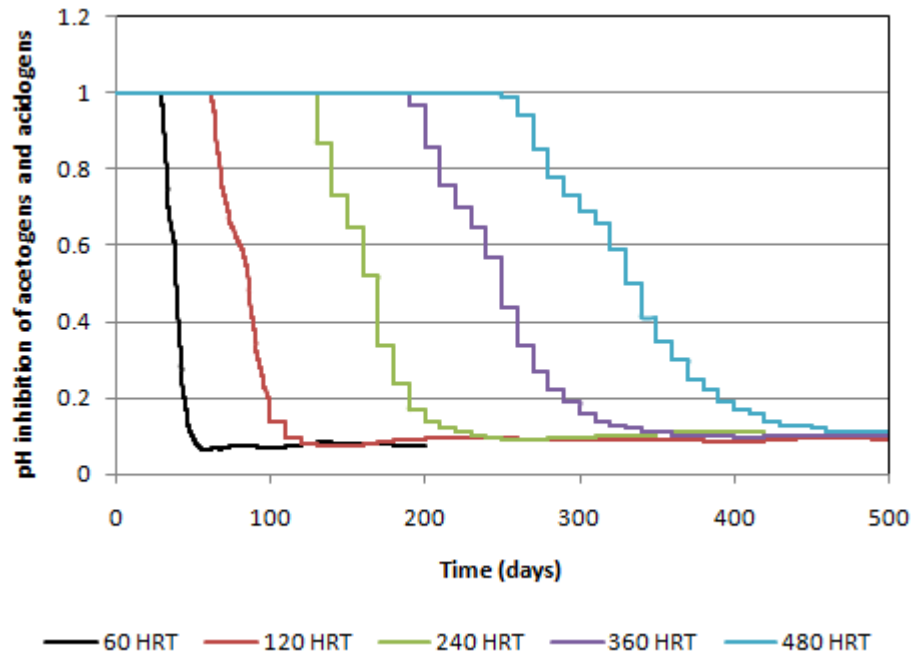


Figure 4-20: pH inhibition of acetogens and acidogens at reactor middle

#### 4.1.6.3 pH inhibition of hydrogen degrading organisms

Hydrogen degrading micro-organisms get severely affected by the decrease of pH in anaerobic digester. Due to high reduction of pH at the reactor front hydrogen degradation organisms get inhibited. It can be shown from the inhibition function of hydrogen degrading organisms and Figure 4-21 shows how it vary with the time at the reactor front. Inhibition of hydrogen degrading organisms all ways occur before the inhibition of acetogens and acidogens and after the inhibition of acetate degrading organisms. Since the rate of decrease of pH at reactor middle is not very much higher as at front, the decrease of inhibition function at the reactor middle is not sharp as that of at reactor front. Figure 4-22 shows the variation of inhibition function at reactor middle under different feed conditions.

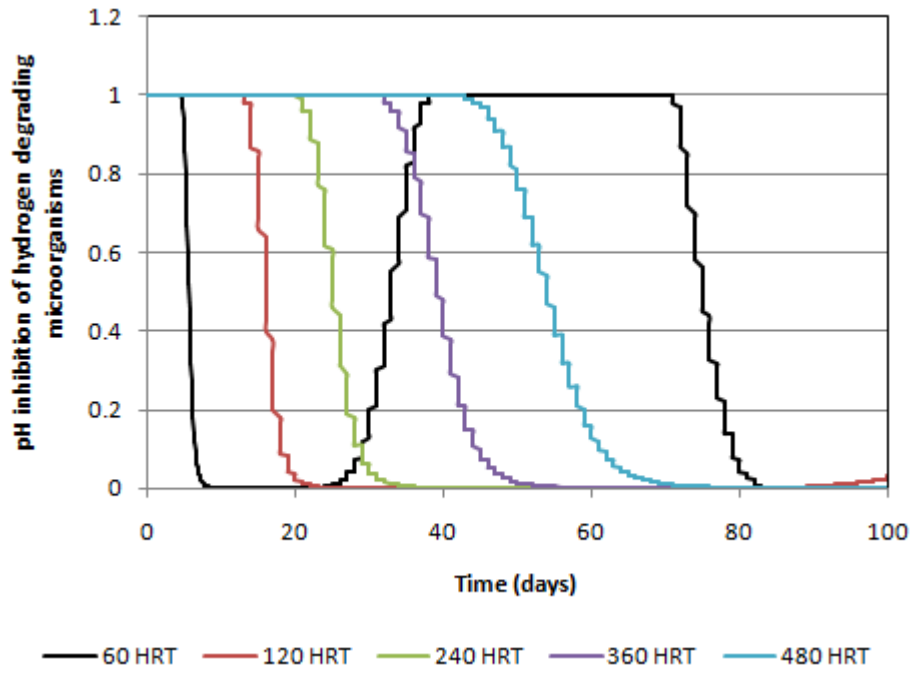


Figure 4-21: pH inhibition of hydrogen degrading microorganisms at reactor front

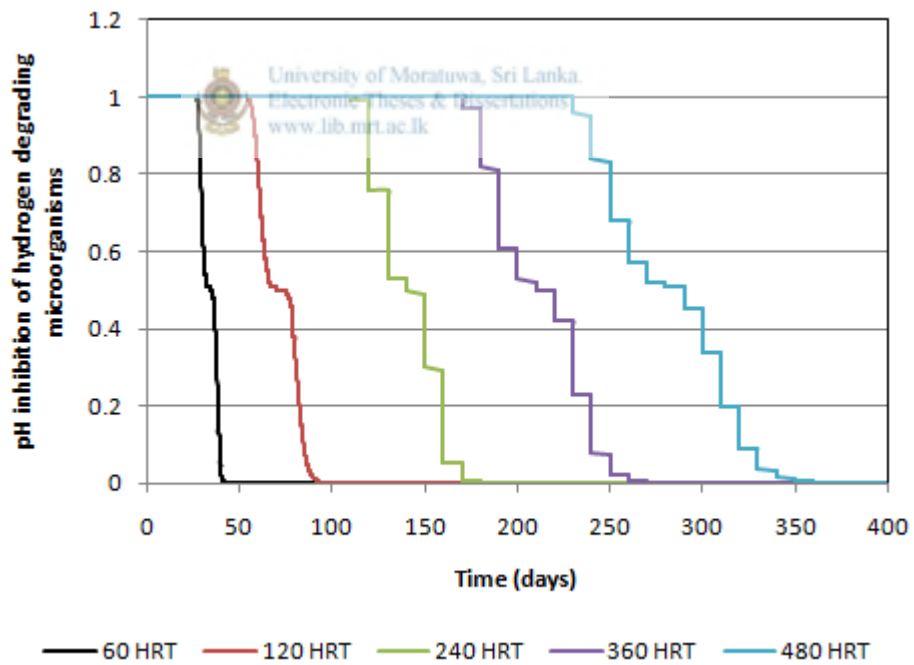


Figure 4-22: pH inhibition of hydrogen degrading microorganisms at reactor middle

A rapid inhibition of methane producing bacteria under high feed rates at the reactor front was observed. Figure 4-17 and Figure 4-21 illustrates the variation of the pH inhibition function of acetate degrading microorganisms and hydrogen degrading microorganisms under different feed rates at reactor front. pH inhibition decreases with the decrease of substrate feed rate. Once methanogenesis process inhibited generation of methane from acetate and hydrogen will terminate in the reactor. There was a maximum value of dissolved methane concentration at any point of the reactor. This maximum concentration starts to decrease with the time as it flows along the reactor with slurry and eventually comes to zero. The highest value of the optimum dissolve methane concentration was observed under a reactor retention time of 60 days and maximum was under retention of 480 days.

#### **4.1.7 Comparison of variations in pH, TVFA and soluble methane along the reactor**

The variation of pH, TVFA and Soluble methane were analyzed at the front, middle and end of plug flow reactor under different feed rates.

##### **4.1.7.1.1 Variations in pH, TVFA and soluble methane along the reactor under 60 days of HRT**

According to the Figure 4-23, rapid pH drop observed at the reactor front under 60 days of HRT. The pH reduction rate reduced along with the reactor length but finally reached to a minimum pH of 4.4.

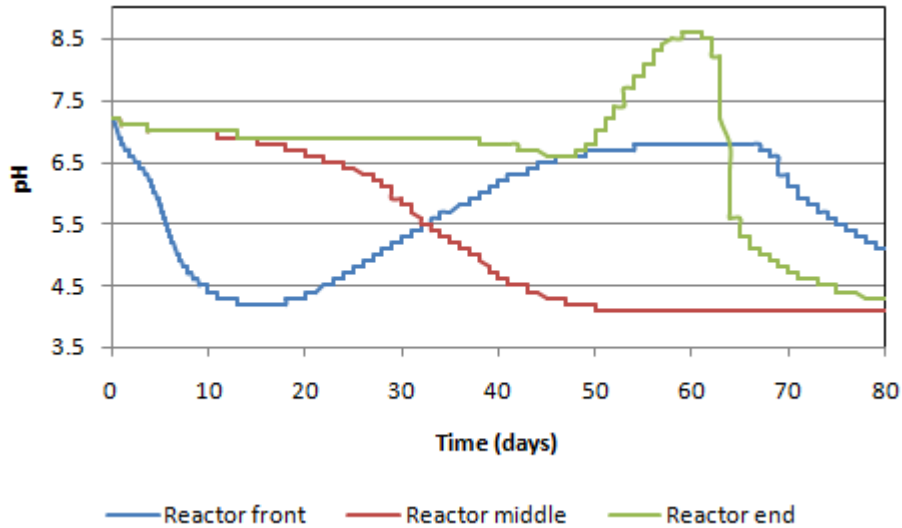


Figure 4-23: pH variation along the reactor under 60 days HRT

Figure 4-24 shows the variation of TVFA along the reactor with 60 days of HRT. At reactor front the maximum TVFA concentration was 0.12 kgCOD/m<sup>3</sup>. The TVFA continuously increased at reactor middle and end. It reached to its maximum steady value of 7.5 kgCOD/m<sup>3</sup> at the reactor middle and end.

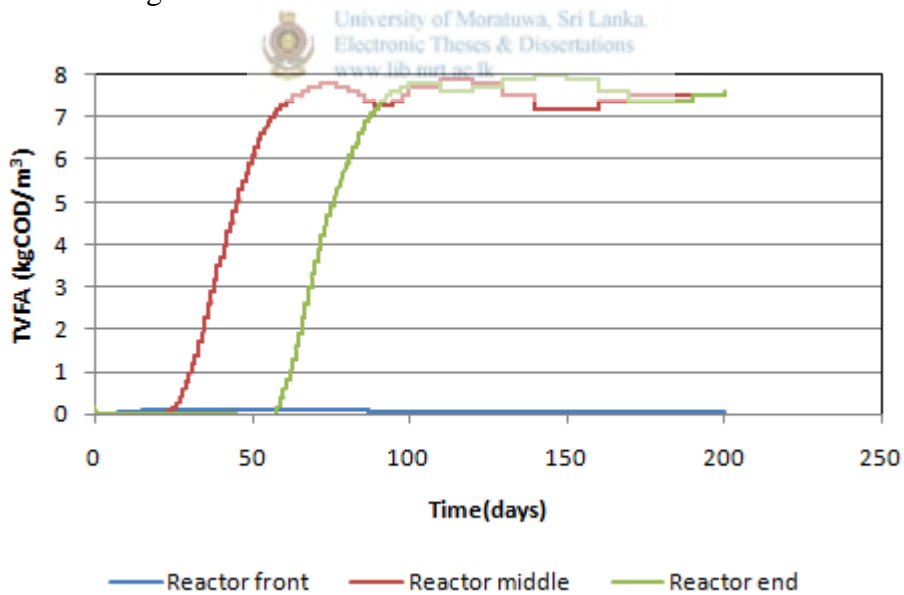


Figure 4-24: TVFA variation along the reactor under 60 days HRT

Figure 4-25 shows the variation of soluble methane along the reactor with 60 days of HRT. At reactor front the maximum soluble methane concentration was 0.03

kgCOD/m<sup>3</sup>. The soluble methane concentration continuously increased at middle and end of the reactor. It reached to its maximum value of 4 kgCOD/m<sup>3</sup> after feed reached to reactor middle. After soluble methane concentration reached its maximum started to decrease continuously and came to zero after 70 days. Similar variation occurred in reactor end as well with concentration of 5.3 kgCOD/m<sup>3</sup>.

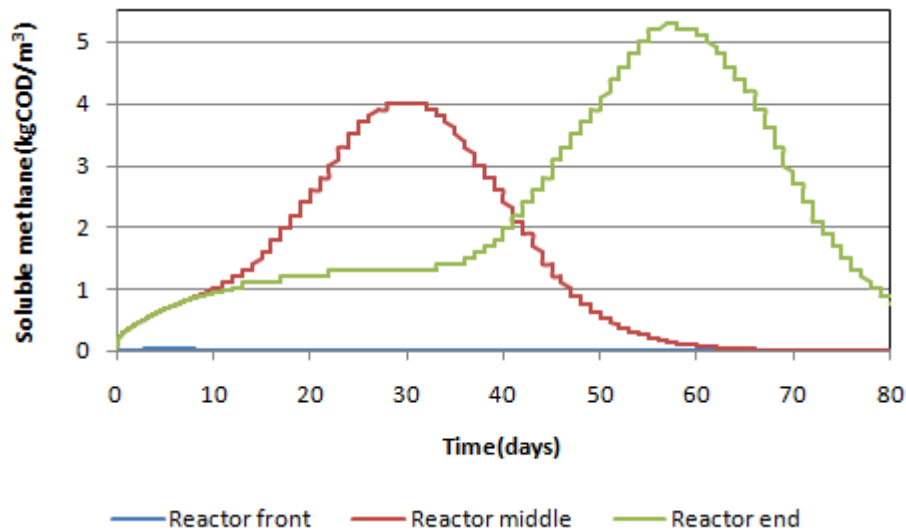


Figure 4-25: Concentration of soluble methane variation along the reactor under 60 days HRT

#### 4.1.7.1.2 Variations in pH, TVFA and soluble methane along the reactor under 120 days of HRT

According to the Figure 4-26, rapid pH drop observed at the reactor front under 120 days of HRT. The pH reduction rate reduced along with the reactor length but finally reached to a minimum pH of 4.2. pH reduction rate has decreased comparatively that of reactor system with 60 days HRT.

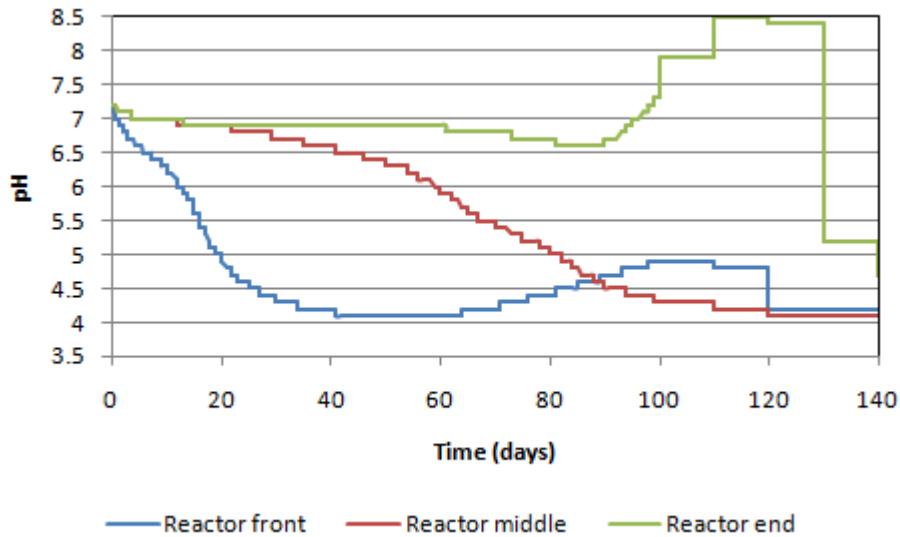


Figure 4-26: pH variation along the reactor under 120 days HRT

Figure 4-27 shows the variation of TVFA along the reactor with 120 days of HRT. At reactor front the maximum TVFA concentration was 0.12 kgCOD/m<sup>3</sup>. The TVFA continuously increased at middle and end. It reached to its maximum steady value of 7.9 kgCOD/m<sup>3</sup> at reactor middle and 8.1 kgCOD/m<sup>3</sup> at reactor end.

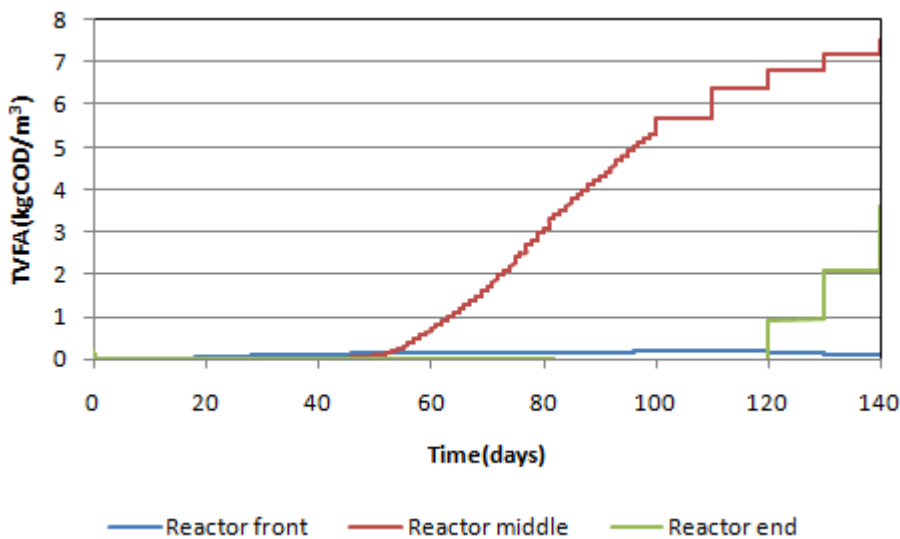


Figure 4-27: TVFA variation along the reactor under 120 days HRT

Figure 4-28 shows the variation of soluble methane along the reactor with 120 days of HRT. At reactor front the maximum soluble methane concentration was 0.07 kgCOD/m<sup>3</sup>. The soluble methane concentration continuously increased at middle and end of the reactor. It reached to its maximum value of 4.6 kgCOD/m<sup>3</sup> at reactor middle. Similar variation occurred in reactor end as well with concentration of 5.9 kgCOD/m<sup>3</sup>. After soluble methane concentration reached its maximum started to decrease continuously and came to zero for every location at the reactor.

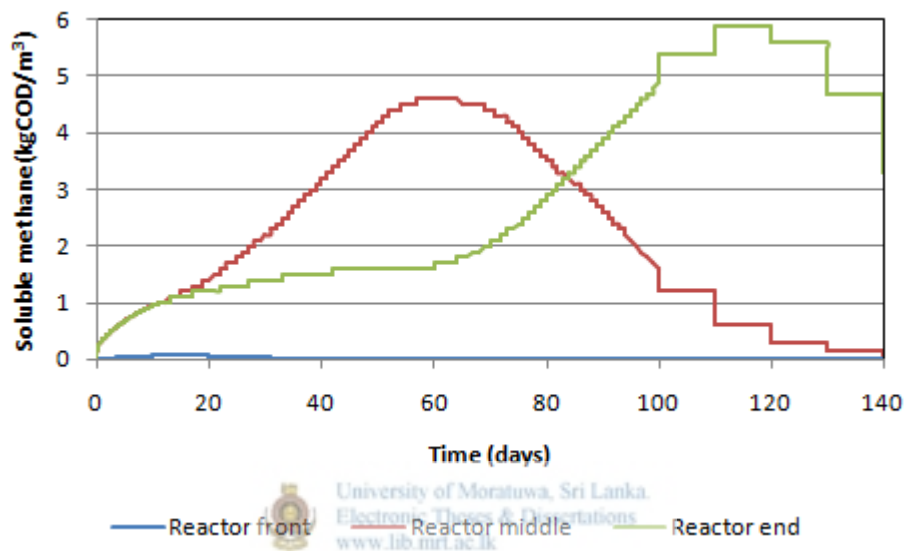


Figure 4-28: Concentration of soluble methane variation along the reactor under 120 days HRT

#### 4.1.7.1.3 Variations in pH, TVFA and soluble methane along the reactor under 240 days of HRT

According to the Figure 4-29, pH variation was observed at the reactor front under 120 days of HRT. Similar variation was observed as under the HRT of 60 and 120 days. pH reached to a minimum value of 4.1 at the reactor front and pH reduction rate has decreased comparatively that of reactor system with 120 days HRT.

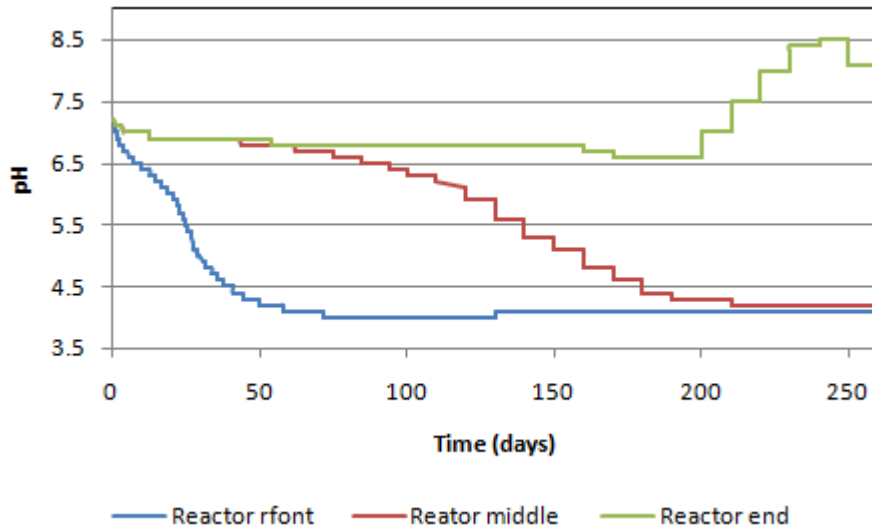


Figure 4-29: pH variation along the reactor under 240 days HRT

Figure 4-30 shows the variation of TVFA along the reactor with 240 days of HRT. At reactor front the maximum TVFA concentration was 0.4 kgCOD/m<sup>3</sup>. The TVFA continuously increased at middle and end the reactor. It reached to its maximum steady value of 8 kgCOD/m<sup>3</sup> at reactor middle and end.

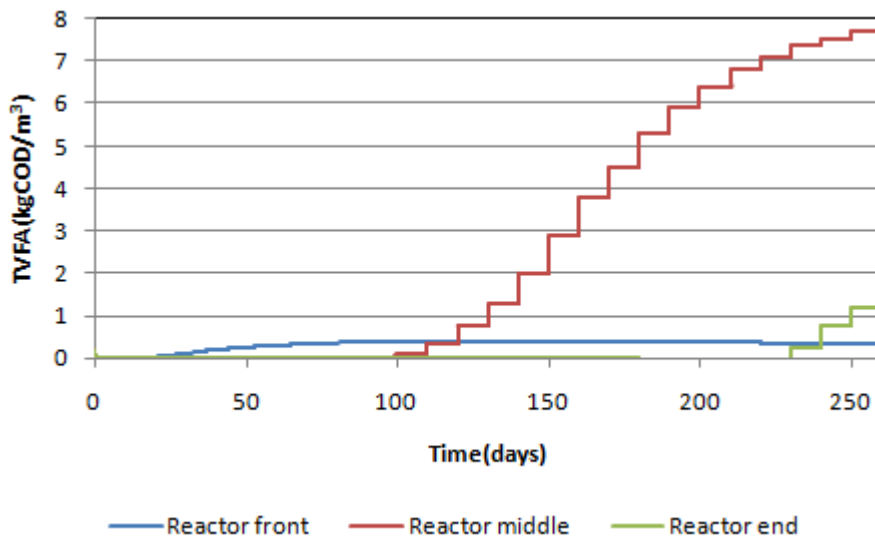


Figure 4-30: TVFA variation along the reactor under 240 days HRT

Figure 4-31 shows the variation of soluble methane along the reactor with 240 days of HRT. At reactor front the maximum soluble methane concentration was 0.21 kgCOD/m<sup>3</sup>. The soluble methane concentration continuously increased as well as at the middle and end of the reactor. It reached to its maximum value of 5 kgCOD/m<sup>3</sup> at reactor middle. Similar variation occurred in reactor end as well with concentration of 5.7 kgCOD/m<sup>3</sup>. After soluble methane concentration reached its maximum started to decrease continuously and came to zero for every location at the reactor.

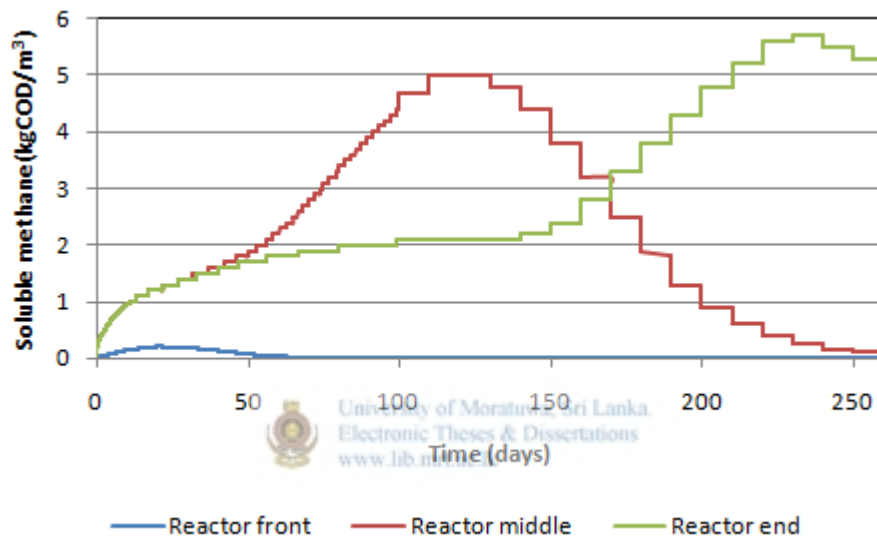


Figure 4-31: Concentration of soluble methane variation along the reactor under 240 days HRT

#### 4.1.7.1.4 Variations in pH, TVFA and soluble methane along the reactor under 360 days of HRT

Figure 4-32 shows the pH variation of the reactor with 360 days of HRT. pH reached to a minimum value of 4 at the reactor front and pH reduction continues at middle and the end as well. At reactor end, pH rose after 290 days and started to reduce when the feed reached the end after 360 days.

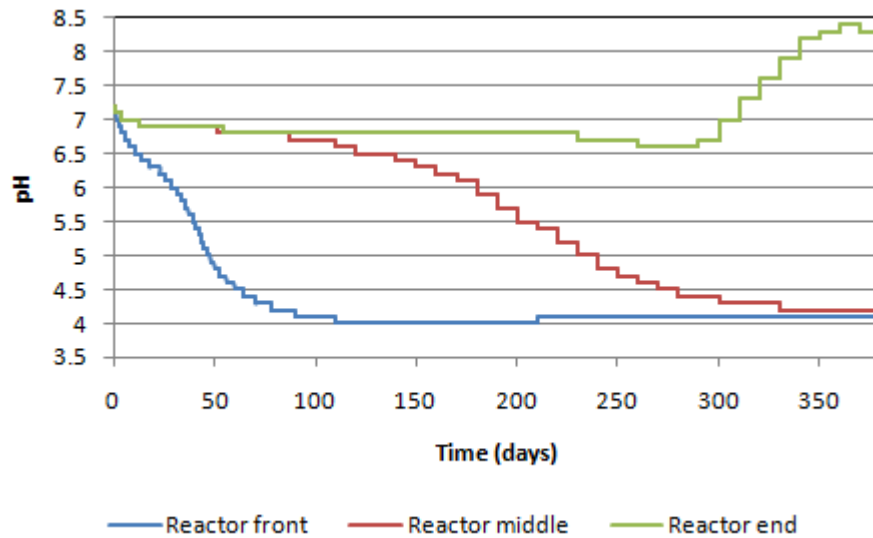


Figure 4-32: pH variation along the reactor under 360 days HRT

Figure 4-33 shows the variation of TVFA along the reactor with 360 days of HRT. At reactor front the maximum TVFA concentration was  $0.6 \text{ kgCOD/m}^3$ . The TVFA continuously increased at middle and end the reactor. It reached to its maximum steady value of  $8 \text{ kgCOD/m}^3$  at reactor middle.

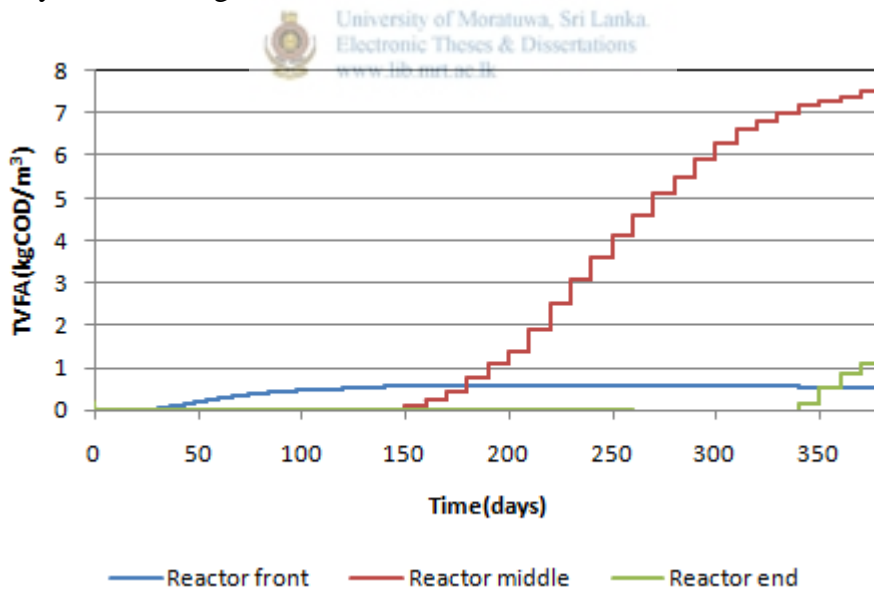


Figure 4-33: TVFA variation along the reactor under 360 days HRT

Figure 4-34 shows the variation of soluble methane along the reactor with 360 days of HRT. At reactor front the maximum soluble methane concentration was  $0.33$

kgCOD/m<sup>3</sup>. The soluble methane concentration continuously increased as well as at the middle and end of the reactor. It reached to its maximum value of 5.1 kgCOD/m<sup>3</sup> at reactor middle. Similar variation occurred in reactor end as well with concentration of 5.6 kgCOD/m<sup>3</sup>. After soluble methane concentration reached its maximum started to decrease continuously and came to zero for every location at the reactor.

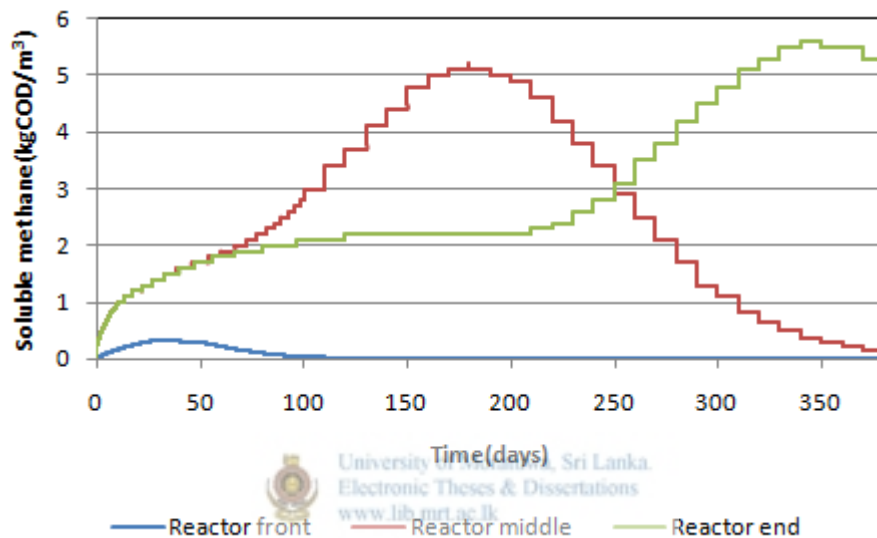


Figure 4-34: Concentration of soluble methane variation along the reactor under 360 days HRT

#### 4.1.7.1.5 Variations in pH, TVFA and soluble methane along the reactor under 480 days of HRT

Figure 4-35 shows the pH variation of the reactor with 480 days of HRT. pH reached to a minimum value of 4 at the reactor front and pH reduction continue at middle and the end as well. At reactor end, pH rose after reactor 370 days and started to reduce when the feed reached the end after 480 days.

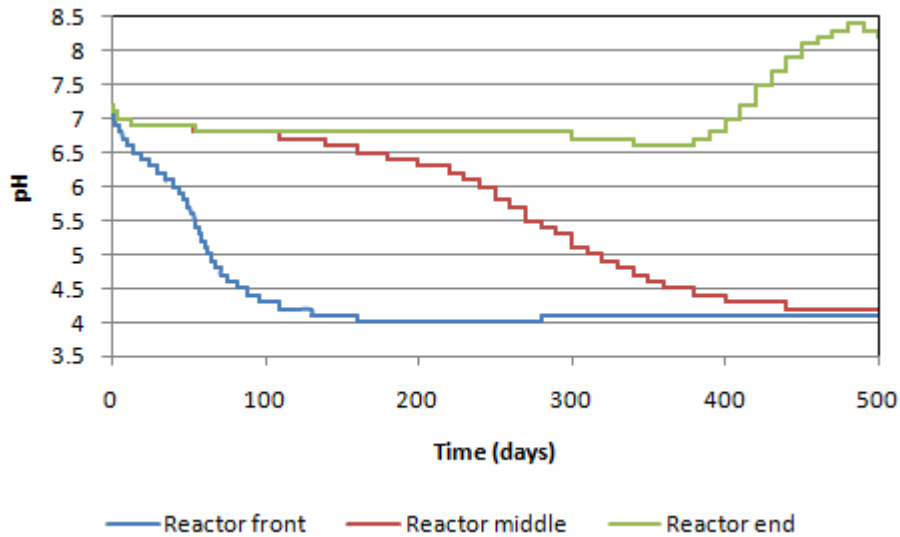


Figure 4-35: pH variation along the reactor under 480 days HRT

Figure 4-36 shows the variation of TVFA along the reactor with 480 days of HRT. At reactor front the maximum TVFA concentration was 0.78 kgCOD/m<sup>3</sup>. The TVFA continuously increased at middle and end of the reactor and came to its optimum value.

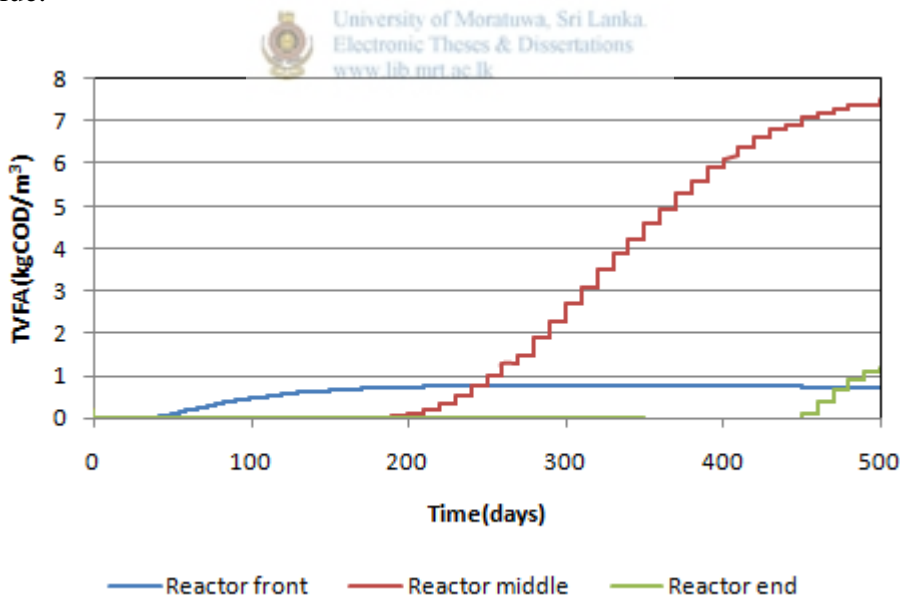


Figure 4-36: TVFA variation along the reactor under 480 days HRT

Figure 4-37 shows the variation of soluble methane along the reactor with 480 days of HRT. At reactor front the maximum soluble methane concentration was 0.46

kgCOD/m<sup>3</sup>. The soluble methane concentration continuously increased as well as at the middle and end of the reactor. It reached to its maximum value of 5.2 kgCOD/m<sup>3</sup> at reactor middle. Similar variation occurred in reactor end as well with concentration of 5.5 kgCOD/m<sup>3</sup>. After soluble methane concentration reached its maximum started to decrease continuously and came to zero for every location at the reactor.

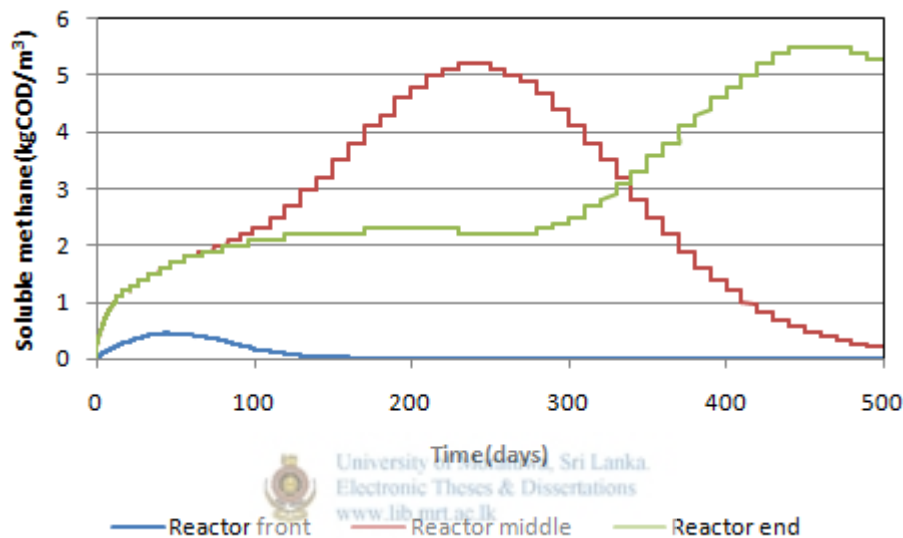


Figure 4-37: Concentration of soluble methane variation along the reactor under 480 days HRT

## 4.2 Results from second plug flow reactor model (2st scenario)

### 4.2.1 Gas production rate

The biogas production rate increase with the increase of retention times in reactors. The reactor system having total retention of 60 days has the least gas production rates and reactor system having that of 480 days has the maximum gas production rate. Higher the retention time the total period of gas production will be increased. Reactor system with 480 days retention produce biogas over almost 150 days and reactor system with 60 days of retention time produced biogas only for 45 days.

According to the results it can be predicted that the biomass will retain in the reactors for low feed rates as retention time increases and system can produce biogas for a longer time before it get inhibited.

Figure 4-38 shows the variation of gas flow with the increase of the feed rate of the reactor system.

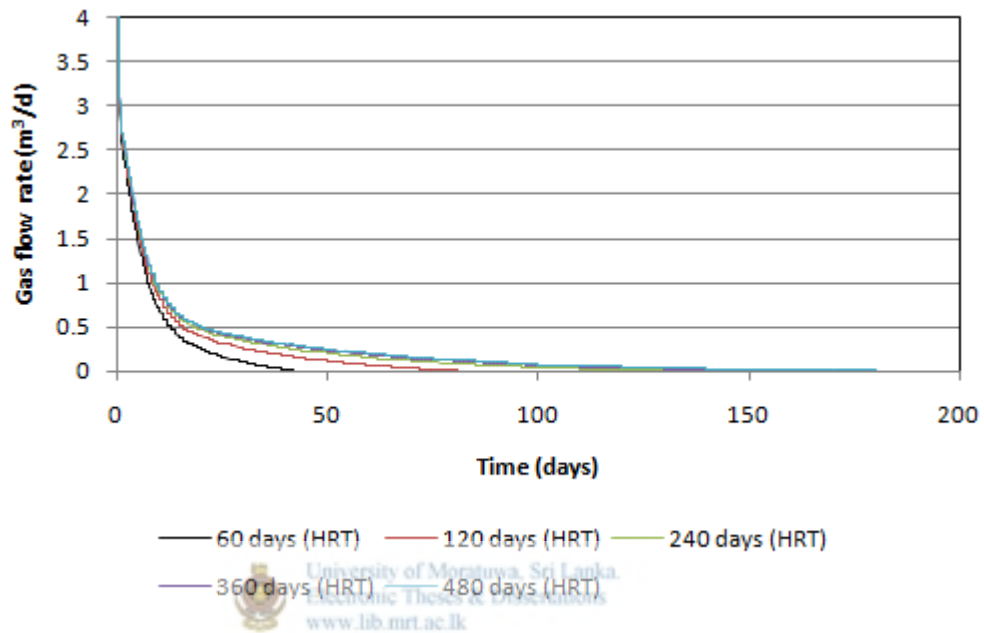


Figure 4-38: Gas production rate under different retention times

#### 4.2.2 Gas composition

The mole percentages of gases in headspace under different retention times are discussed below.

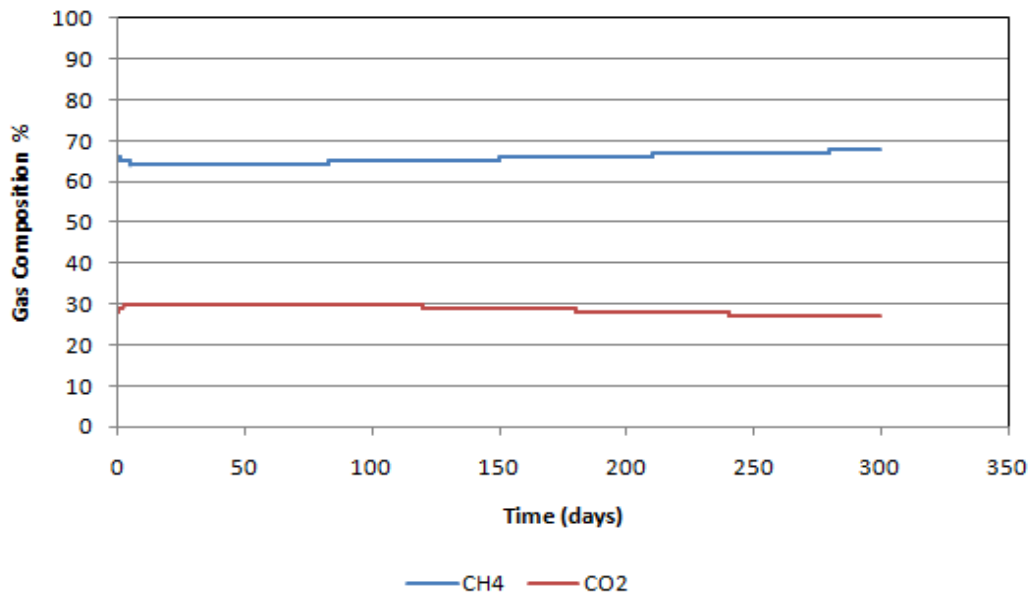


Figure 4-39: Variation of gas composition in headspace with 480 HRT



Figure 4-39 illustrates the percentages of gases in headspace when the reactors are operated at retention of 480 days. As in the figure, there is a sudden variation of mole percentages of biogas at the beginning of the digestion. There the CH<sub>4</sub> percentage drops drastically until it comes to a value of 63 %. Mean while the CO<sub>2</sub> percentage increases until 30 % and this continues for 100 days. After 100 days the mole percentage of CH<sub>4</sub> starts to increase gradually and subsequently CO<sub>2</sub> percentage decreases. This variation continues for a long period of time approximately 250 days. When the system gets inhibited the gas production stops and mole percentages became constant.

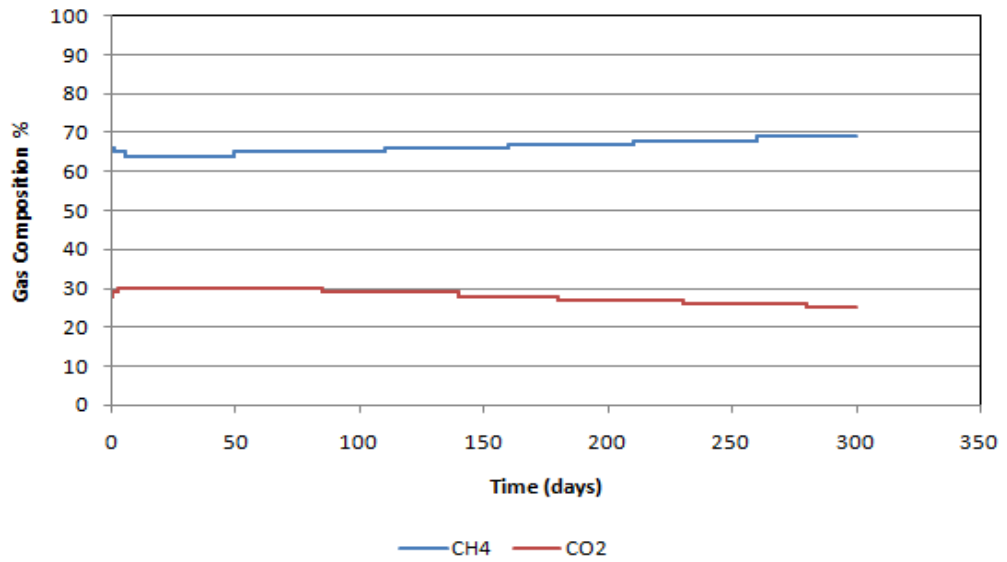


Figure 4-40: Variation of gas composition in headspace with 360 HRT

Figure 4-40 illustrates the percentages of gases in headspace when the reactors are operated at retention of 360 days. Here the mole percentage shows almost same variation comparing with Figure 4-39 which corresponds to 480 days of retention.

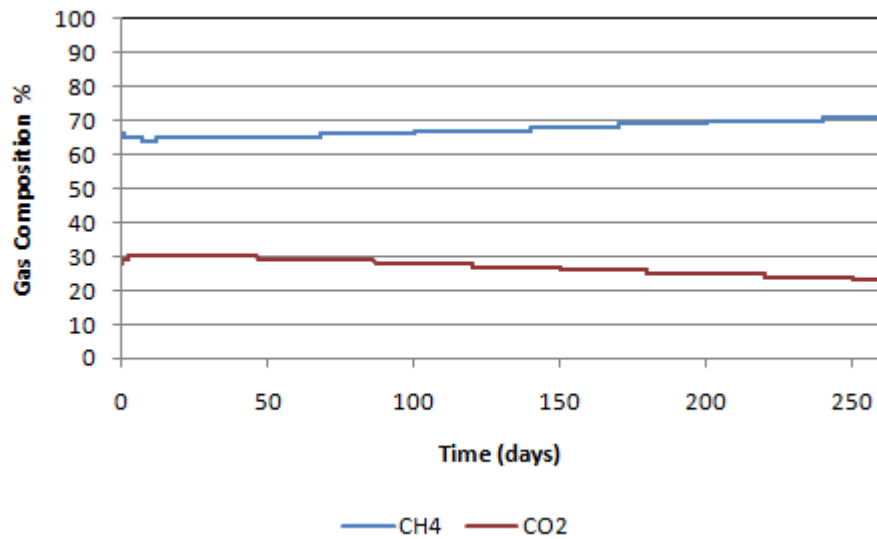
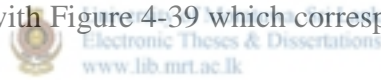


Figure 4-41: Variation of gas composition in headspace with 240 HRT

With the decrease of the retention time the reactors get inhibited in less period of time. Accordingly the time of gas production decreases and it can be illustrated by Figure 4-40. Here the gas production from the reactor system completely stops around 100 days. Even though it inhibits at 100 days, the produced gases which are in dissolve state in reactors diffused to the headspace. Thus the mole percentages continue to increase beyond 100 days and eventually come to a steady level around 300 days as shown in Figure 4-42.

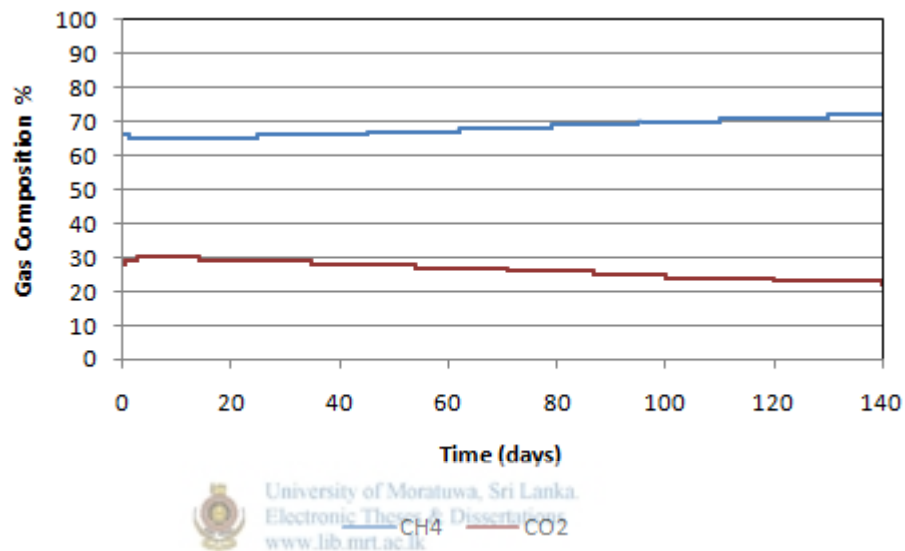


Figure 4-42: Variation of gas composition in headspace with 120 HRT

Further reduction of retention time in the reactor system result an inhibition with in short time. With the time all the gases dissolved in the liquid media diffuse in to the headspace. Figure 4-43 shows the mole percentages of gases in the reactor system having 60 HRT.

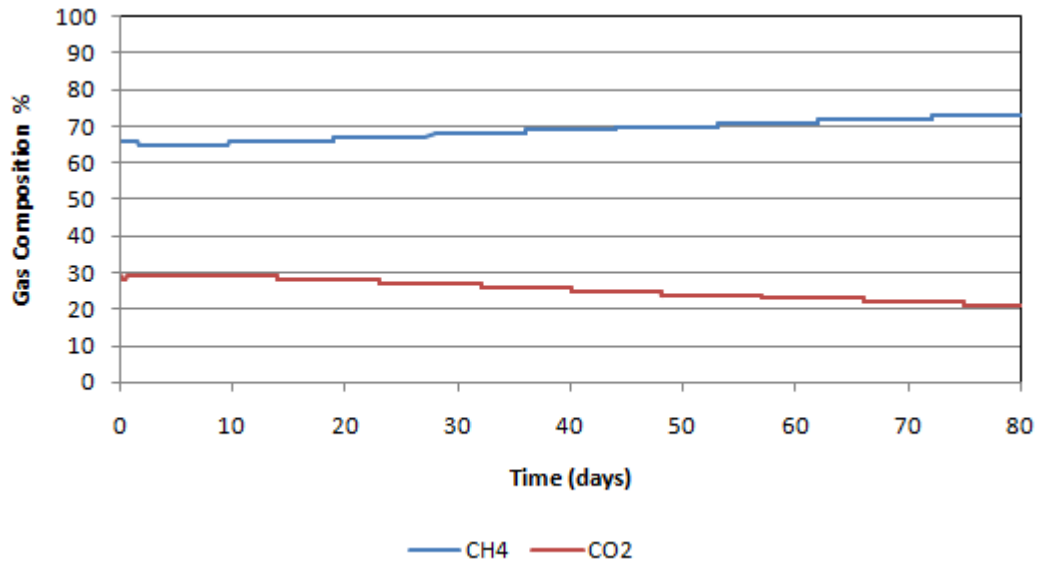


Figure 4-43: Variation of gas composition in headspace with 60 HRT

#### 4.2.3 Variation of pH in the first reactor

The variation of the pH in the first reactor was observed for each retention time and showed in the figure 4-44. Under low retention time high amount of substrate is fed in to the reactor. Thus the rate of VFA formation is high in this condition. Further under a low retention time there will be high amount of wash out of biomass out of the reactor system. Thus when the methanogenesis washed out there will not have adequate microorganisms to consume the VFA formed. Therefore there will be an accumulation of VFA in the reactor. This will leads to sudden pH drop in first reactor.

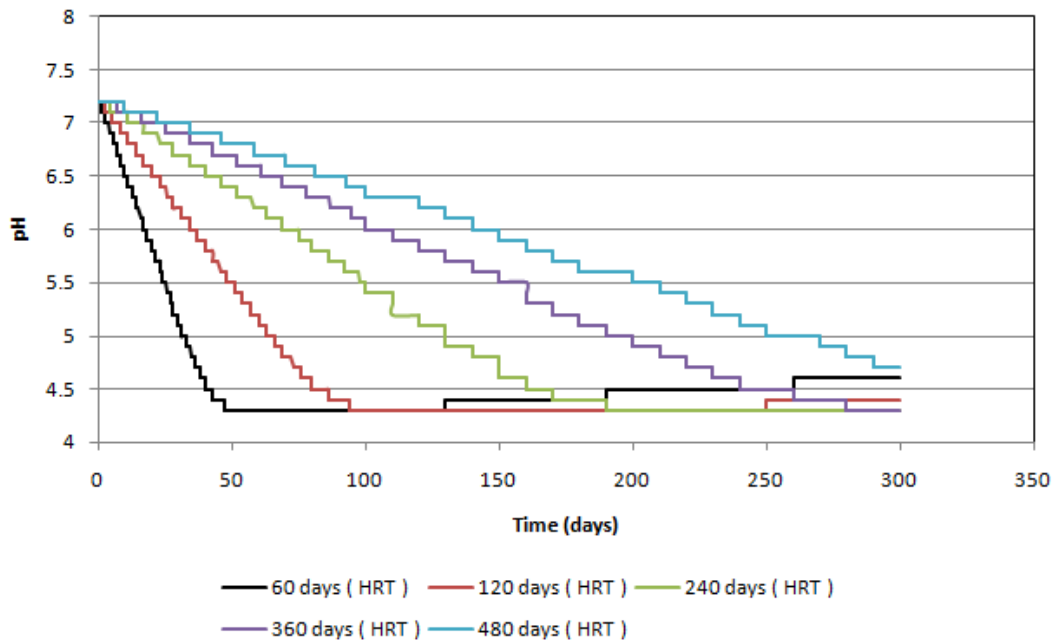
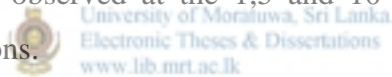


Figure 4-44: Variation of pH in first CSTR

#### 4.2.4 Variation of pH along the CSTR series under different feed rates

Variation of pH was observed at the 1<sup>st</sup> and 10<sup>th</sup> reactor of CSTR series under different feed conditions.



##### 4.2.4.1 Variation of pH along the CSTR series under 60 days of HRT

Figure 4-45 illustrate the variation of pH along the CSTR series under 60 days of HRT. According to the Figure 4-45, a sudden pH drop was observed at the first reactor. With the increase of reactor HRT this pH drop reduced. For every feed rate pH changed from 7.3 to 4.3 and eventually remained at 4.3. At the 5<sup>th</sup> and 10<sup>th</sup> reactors, variations of pH are similar to that of 1<sup>st</sup> reactor. In 5<sup>th</sup> and 10<sup>th</sup> reactors, decrease of pH reduced comparative to the 1<sup>st</sup> CSTR.

At high feed rates the rate of VFA formation is high. As a result of that simulation results shows a rapid pH drops at the first reactor.

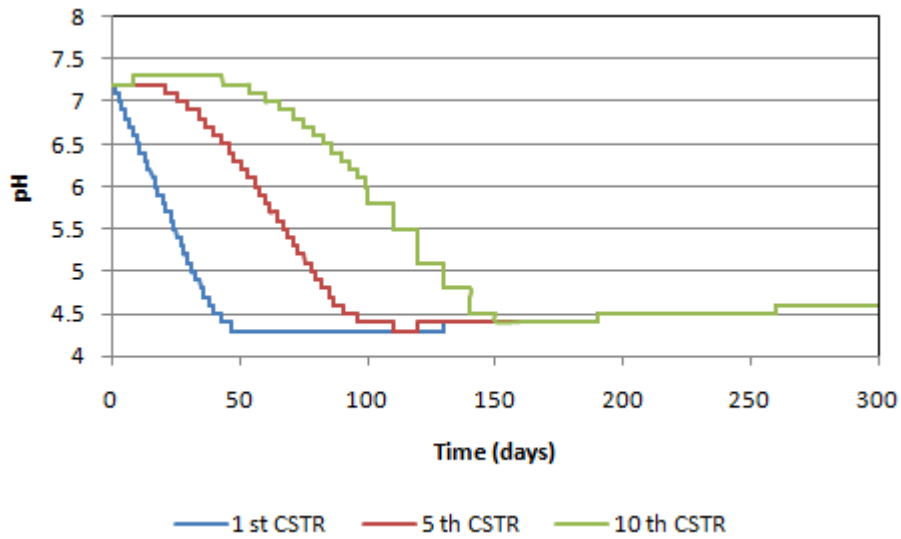


Figure 4-45: Variation of pH along the CSTR series under 60 days of HRT

#### 4.2.4.2 Variation of pH along the CSTR series under 120 days of HRT

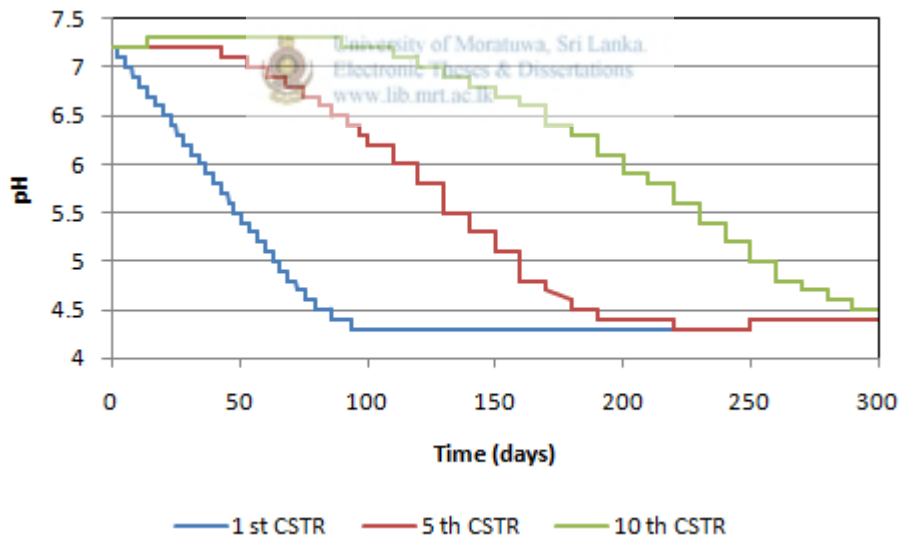


Figure 4-46: Variation of pH along the CSTR series under 120 days of HRT

#### 4.2.4.3 Variation of pH along the CSTR series under 240 days of HRT

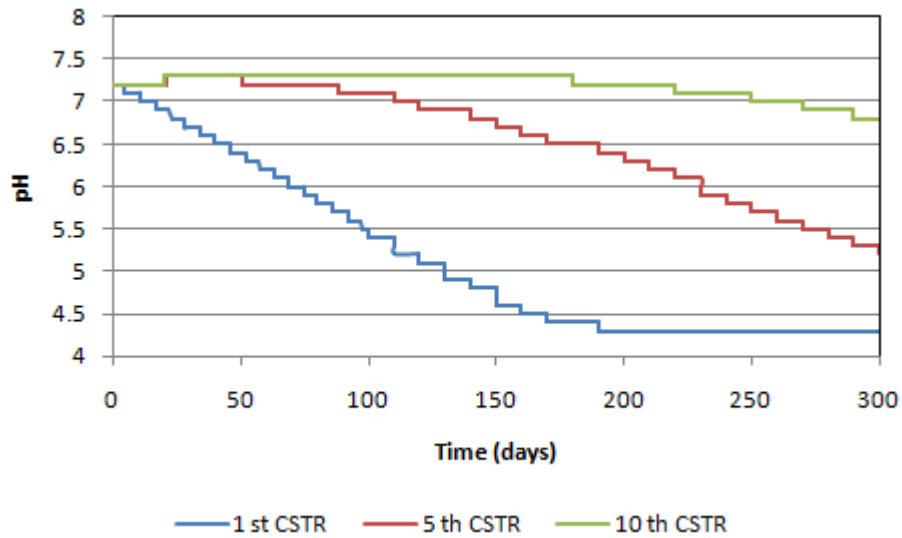


Figure 4-47: Variation of pH along the CSTR series under 240 days of HRT

#### 4.2.4.4 Variation of pH along the CSTR series under 360 days of HRT

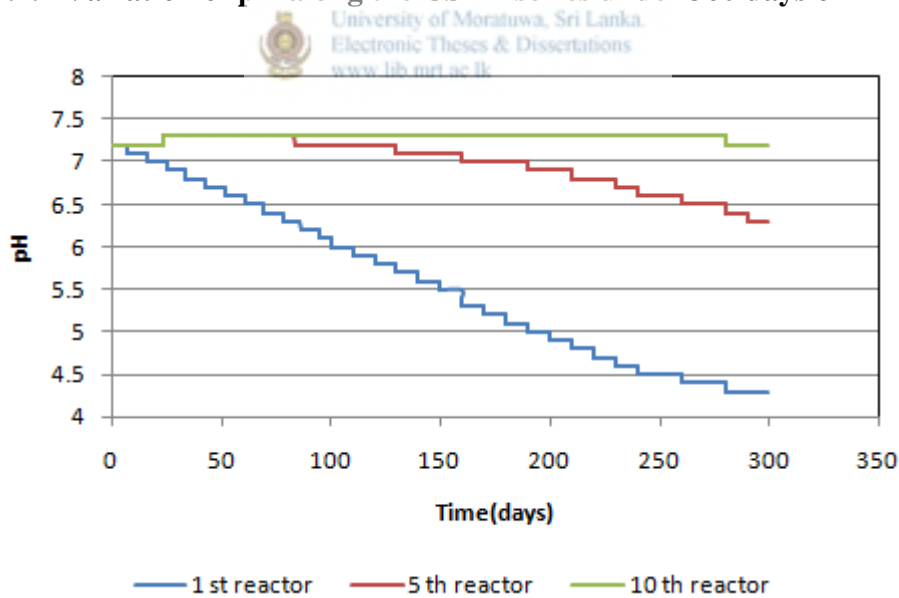


Figure 4-48: Variation of pH along the CSTR series under 360 days of HRT

#### 4.2.4.5 Variation of pH along the CSTR series under 480 days of HRT

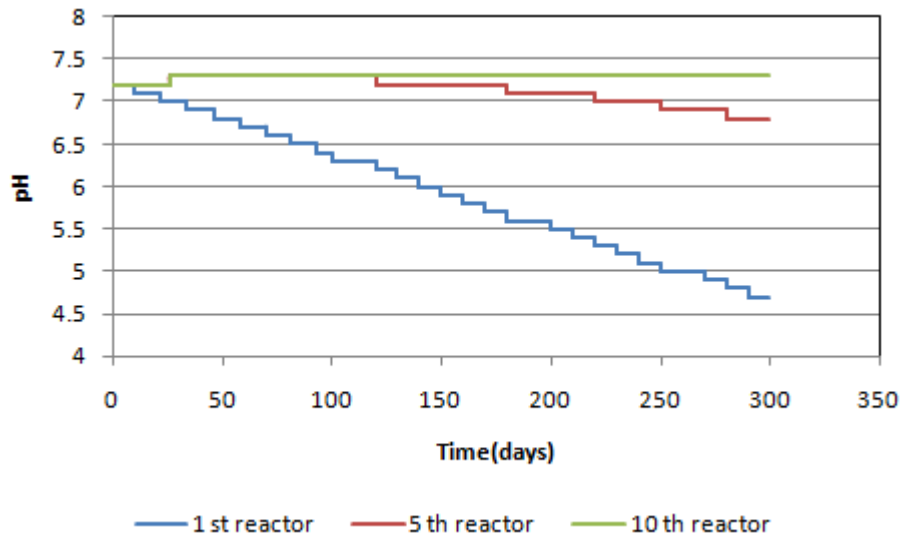


Figure 4-49: Variation of pH along the CSTR series under 480 days of HRT

#### 4.2.5 Variations in inhibition functions of the reactor



As in the section 4.1.6, reactor inhibitions were analyzed in the first reactor of the CSTR series. There a severe pH inhibition of microorganisms was observed in the first reactor under different reactor feed rates. Figure 4-50 shows the variation of pH inhibition function of acetate degrading microorganisms. According to the Figure 4-44 pH of the reactor reduced rapidly under low HRT. Consequently a rapid inhibition was observed in acetate degrading microorganisms under low HRT. The inhibition reduced with the increase of reactor HRT. Although it was improved all inhibition functions of acetate degrading microorganisms came to zero after a period of time.

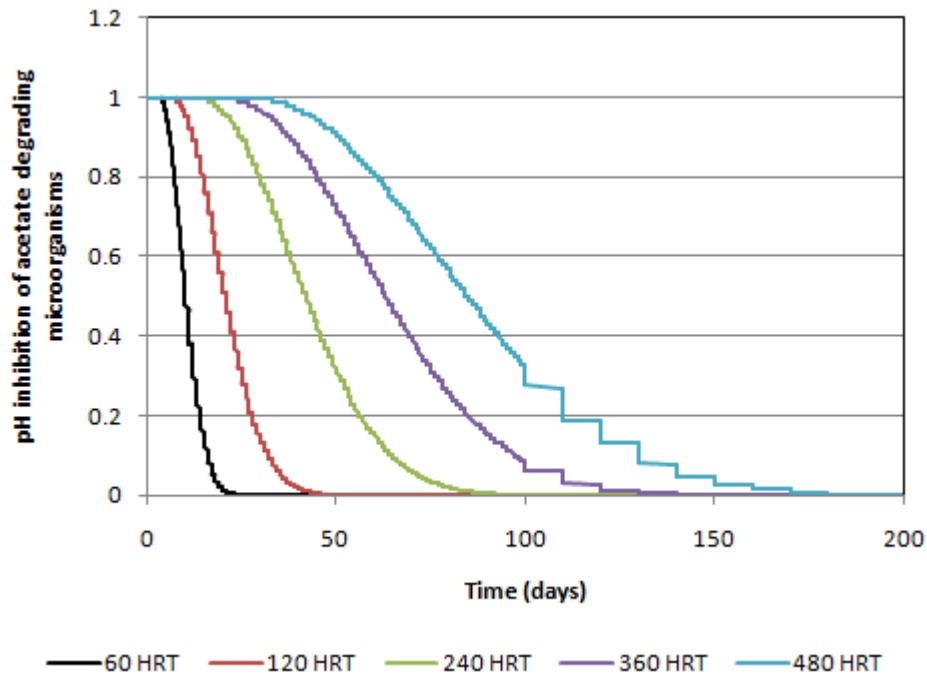


Figure 4-50: pH inhibition of acetate degrading microorganisms

Figure 4-51 illustrate the pH inhibition of hydrogen degrading microorganisms. Here the variation is similar to the pH inhibition of acetate degrading microorganisms. Sudden pH variation in first reactor has resulted in inhibition of methanogenic bacteria.

pH inhibition of acidogenic and acetogenic microorganisms are shown in the Figure 4-52. Due to the pH drop in first reactor rapid inhibition can be observed in acidogenic and acetogenic microorganisms. There was an inhibition improvement showed in reactor HRT values of 60 and 120 days. The value of the inhibition function increases after 60 days in 60 HRT reactor system and 100 days of 120 HRT reactor systems. Other inhibition functions correspond to 240, 360, and 480 HRT became to a steady value of 0.15 throughout the reactor simulation.

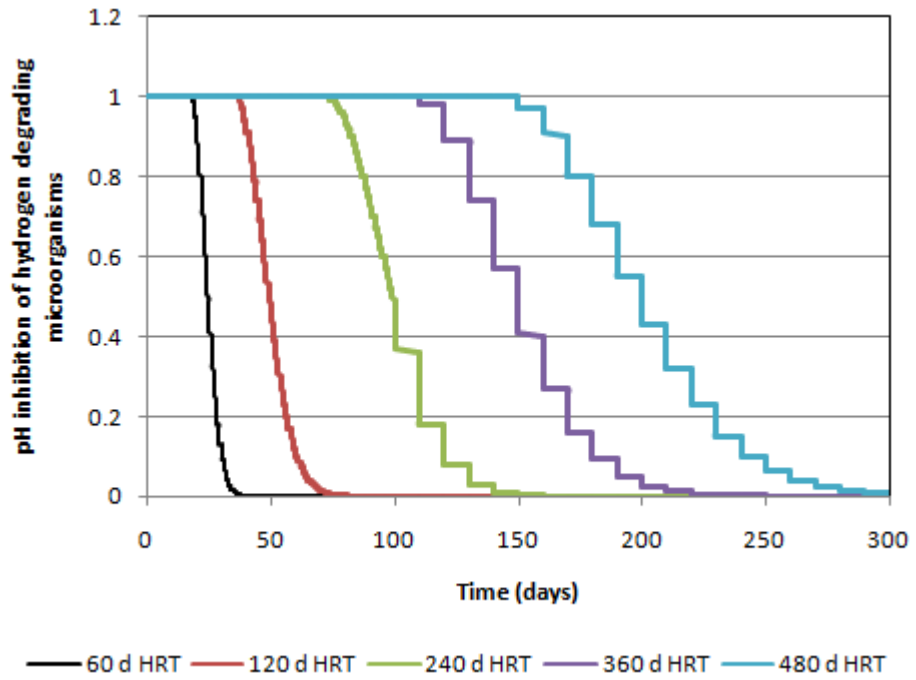


Figure 4-51: pH inhibition of hydrogen degrading microorganisms

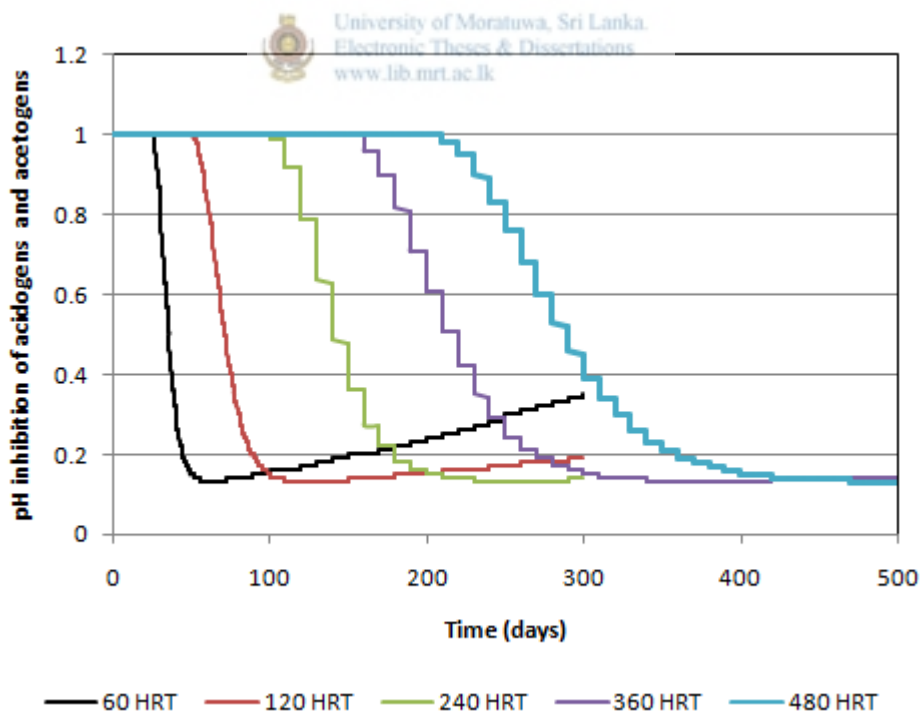


Figure 4-52: pH inhibition of acidogens and acetogens